

Lindgren
WITHDRAWN
MASS. INST. TECH.
AUG FROM
MIT LIBRARIES

A FLUME STUDY OF RIPPLE GROWTH
IN FINE SAND

by

JOHN R. DINGLER

Submitted in Partial Fulfillment
of the Requirements for the
Degree of Master of Science

at the

MASSACHUSETTS INSTITUTE OF TECHNOLOGY

June, 1968

Signature of Author:
Department of Geology and
Geophysics
May 17, 1968

Certified by:
Thesis Supervisor

Accepted by:
Head of Department

ABSTRACT

A FLUME STUDY OF RIPPLE GROWTH IN FINE SAND

by

John R. Dingler

Submitted to the Department of Geology and Geophysics on May 17, 1968, in partial fulfillment of the requirements for the degree of Master of Science.

A recirculating flume 20' long by 6.5" wide by 13" deep was used to study ripple propagation downstream of a small mound manufactured on a bed of very fine sand ($d_m = 0.125$ mm). The mounds were of finite width and varying relative height h/y_o . The shape of the resulting crests was studied and an explanation offered for the three-dimensional nature of the crests. Ripple propagation was also investigated when the flow was less than that necessary to move the grains as bed load. The crest shape of the first few crests formed in each run was two-lobed, with a transverse crest separating the lobes. Scour was strongest behind the two lobes. The ripple shape was attributed to finite width of the mound which produced a transverse velocity component downstream of the mound. Ripple growth was characterized by crest spacing s_i vs. time for the first three or four spacings ($i = 1, 2, 3,$ and 4 respectively). Growth was rapid at first, but eventually decreased to a linear rate. Reproducibility was very good for s_1 but decreased as i increased. The growth rate increased for both increasing Re_p and h/y_o . When $Re_p < Re_{pc}$, ripples propagated if the relative mound height was large enough. This is contrary to the statements of most authors who believe that a rippled bed will become flat if Re_p becomes less than Re_{pc} .

Thesis Supervisor: Prof. John B. Southard

Department of Geology and Geophysics
Massachusetts Institute of Technology
Cambridge, Massachusetts 02139
May 17, 1968

Professor Edward N. Hartley
Secretary of the Faculty
Massachusetts Institute of Technology
Cambridge, Massachusetts 02139

Dear Professor Hartley:

In accordance with the regulations of the Faculty, I herewith submit a thesis, entitled "A Flume Study of Ripple Growth in Fine Sand," in partial fulfillment of the requirements for the degree of Master of Science in Geology and Geophysics at the Massachusetts Institute of Technology.

Respectfully submitted, / /

John R. Dingler /

TABLE OF CONTENTS

	Page
INTRODUCTION	8
General	8
Background	10
Objective	19
Acknowledgements	20
APPARATUS	21
Flume	21
Carriage	23
Sand	25
PROCEDURE	28
RESULTS	33
DISCUSSION OF RESULTS	46
Crest Shape	46
Ripple Growth; $1.66 < Re_p < 2.50$	52
Ripple Growth; $Re_p < Re_{pc}$	59
CONCLUSIONS	61
SUGGESTIONS FOR FUTURE WORK	62
SUMMARY	63
APPENDIX	68
A Notation	68
B Orifice Calibration	70
C Summary of Data	72
BIBLIOGRAPHY	82

LIST OF FIGURES

<u>Number</u>	<u>Title</u>	<u>Page</u>
1a	Liu curve with transposed Shields curve	15
1b	Shields Diagram	15
2	Relationship of bed forms to flow regime for fine sand	16
3	Recirculating flume	22
4	Instrument carriage	24
5	Sieve analysis	26
6	Photomicrograph of the sand	27
7	Mound at time zero	30
8	Crest spacing s vs. time for Run 1 $s_{n=4}$, $Re_p = 2.15$, $h/y_o = 0.071$	35
9	Crest spacing s vs. time for Run 2 $s_{n=4}$, $Re_p = 2.15$, $h/y_o = 0.071$	36
10	Crest spacing s vs. time for Run 3 $s_{n=4}$, $Re_p = 2.15$, $h/y_o = 0.071$	37
11	Crest spacing s vs. time for Run 4 $s_{n=3}$, $Re_p = 1.74$, $h/y_o = 0.062$	38
12	Crest spacing s vs. time for Run 5 $s_{n=4}$, $Re_p = 1.74$, $h/y_o = 0.08$	39
13	Crest spacing s vs. time for Run 6 $s_{n=4}$, $Re_p = 1.74$, $h/y_o = 0.107$	40
14	Crest spacing s vs. time for Run 7 $s_{n=4}$, $Re_p = 1.73$, $h/y_o = 0.091$	41
15	Crest spacing s vs. time for Run 8 $s_{n=4}$, $Re_p = 2.04$, $h/y_o = 0.090$	42
16	Crest spacing s vs. time for Run 9 $s_{n=4}$, $Re_p = 2.25$, $h/y_o = 0.089$	43
17	Crest spacing s vs. time for Run 11 $s_{n=3}$, $Re_p = 1.43$, $h/y_o = 0.23$	44

LIST OF TABLES

<u>Number</u>	<u>Title</u>	<u>Pages</u>
1	Flow conditions and mound geometries for the runs	34
2	Change in growth rate for variable Re_p and constant h/y_o	57
3	Summary of data - Run 1	72
4	Summary of data - Run 2	73
5	Summary of data - Run 3	74
6	Summary of data - Run 4	75
7	Summary of data - Run 5	76
8	Summary of data - Run 6	77
9	Summary of data - Run 7	78
10	Summary of data - Run 8	79
11	Summary of data - Run 9	80
12	Summary of data - Run 10	81

LIST OF FIGURES (continued)

<u>Number</u>	<u>Title</u>	<u>Page</u>
18	Crest height vs time for Run 10 Crests 1 - 4, $Re_p = 1.77$	45
19a-f	Stages of ripple growth below mound	49
20	Growth of a rippled bed; typical "v" shape	49
21a,b	Propagation of asymmetry	49
22	Cross-section showing shape of transverse crest	50
23	Flume coordinate system	51
24	Reproducibility of s_1 for different runs	54
25	Reproducibility of s_2 for different runs	55
26	Reproducibility of s_3 for different runs	56
27	Variations in s_1 for variable h/y_0 and constant Re_p	58
28	Effects of relative mound height on ripple propagation	60
29	Typical two-lobed ripple with transverse crest	65
30	Growth of crest spacing s with time	66
31	Regions of ripple propagation	67
32	Orifice calibration	71

INTRODUCTION

General

Knowledge of the formation and preservation of bed forms is of interest to both geologists and hydraulic engineers. Geologists use the preserved bed forms --ripple marks and cross-bedding-- and associated sedimentary structures in interpreting ancient environments, while hydraulic engineers use information on alluvial channel resistance in order to properly design channels and to predict sediment transport rates.

Ripples form in noncohesive sediments under flow conditions prevalent in nature. Geologists have long recognized their usefulness as indicators of bedding sequence and current direction, but only recently have they realized that ripple marks might also be used to interpret the paleo-flow regime; comparison of bed forms found in the field with bed forms produced in controlled flume experiments should help in such interpretations.

Ripple marks are primary sedimentary structures which form as quasi-periodic undulations on a sedimentary surface due to fluid motion. To some extent they characterize the kind of fluid --air and water being the two types of fluids encountered in nature-- and the kind of fluid motion acting on the bed -- gravity waves or unidirectional currents. Except in spe-

cial cases (Inman and Bowen, 1963), flume studies have been concerned with water-formed current ripples. These are characterized by asymmetrical shape, with a long, gentle stoss slope and a shorter, steeper lee slope.

Hydraulic engineers are interested in the sediment-transport and flow-resistance characteristics of ripples. The friction factor for a rippled bed is five to six times larger than that for a flat bed at the same shear velocity. Thus, design of earth channels and prediction of sediment transport rates in rivers depends largely on ability to predict the bed configuration.

Hydraulic engineers have studied ripple properties in controlled experiments in laboratory flumes. Two kinds of flumes are in general use: recirculating flumes, which recycle both sediment and water, and once-through flumes, to which sediment and water must be added continuously at the upstream end. Except for small variations attributable to flume design, flumes can accurately reproduce conditions found in nature. From these studies much information has been collected on sediment transport and changes in flow resistance due to the formation and growth of ripples (for example, Barton and Liu (1955), Brooks (1958), Colby (1961), Simons and Richardson (1962) and Hill (1965)). Some work has been done on predicting ripple initiation (for example, Shields (1936), Rubey (1948), and Liu (1957)), but this aspect

of ripples is still poorly understood. Much of the problem here is due to an inability to predict the role of turbulence at the water-sediment boundary in initiation of motion.

Background

The concept of a turbulent boundary layer and a laminar sublayer was introduced by Prandtl (Schlichting, 1960). Next to the fluid-bed boundary layer there is a region of laminar flow where viscous effects predominate over turbulent effects. The thickness of the laminar sublayer, δ , is proportional to ν / U_* where

- $\nu = \mu / \rho$ is the kinematic viscosity.
- ρ is the fluid density.
- μ is the absolute viscosity.
- $U_* = (\tau_0 / \rho)^{1/2}$ is the shear velocity.
- $\tau_0 = gRS$ is the bed shear stress.
- g is the acceleration due to gravity.
- R is the hydraulic radius of the channel.
- R is taken to be equal to the mean depth, y_0 , in this study.
- S is the slope of the energy gradient and is approximately equal to the bed slope.

Outside the laminar sublayer turbulent shear effects predominate over viscous ones with the result that eddies form and fluid mixing is greatly enhanced.

If the thickness of the laminar sublayer is greater than the size of any protrusions at the boundary, the boundary is called smooth. Correspondingly, if the protrusions extend through the laminar sublayer, the boundary is called rough. There is a transition region

where only some of the bed elements protrude into the turbulent boundary layer.

The usual method of characterizing the three types of boundaries is in terms of a particle Reynolds number Re_p :

$$Re_p = k_s U_* / \nu \quad (1)$$

where k_s is the hypothetical roughness elevation according to Nikuradse (Schlichting, 1960) and is approximately equal to the mean sand diameter d_m . These roughness relations were developed from pipe-flow data, but they are applicable to open channels if four times the hydraulic radius is substituted for the pipe diameter in all the pertinent equations. The three regions are delineated as follows:

$$\begin{aligned} \text{smooth:} & \quad d_m U_* / \nu < 3, \\ \text{transition:} & \quad 3 < d_m U_* / \nu < 70, \\ \text{turbulent:} & \quad d_m U_* / \nu > 70. \end{aligned}$$

Einstein (1942) suggested that a bed hydraulic radius, R_b , be used instead of the total hydraulic radius. R_b is essentially a correction for sidewall roughness, and its value approaches y_0 for smooth walls and a small depth-to-width ratio. As both these conditions were met in this study, y_0 was used in all cases where the hydraulic radius term appeared.

The number of experimental studies on flow resis-

tance and grain motion is far too large to permit discussion of all of them. A few of the more pertinent ones will be discussed below. Chien (1957) gave a good summary of work done up to 1957, while the ASCE Task Committee on Preparation of Sedimentation Manual (1966) covered work through 1966. Plate (1957) gave a good summary of foreign work through 1957.

The first definitive work on sediment transport in alluvial channels was by Gilbert (1914). Using a wooden flume 31.5 ft. long by 1.96 ft. wide, the capacity for hydraulic traction was compared with slope, depth and width of current, and particle size. He used both uniform and mixed materials. Traction is the term that he used for bed-load movement. In conjunction with transport by traction, he discussed saltation and the forces and conditions necessary for particle movement.

First of all, he assumed that the flow is turbulent, since laminar flow is impossible with velocities competent for traction. He hypothesized that the saltated grains are given an upward lift by pivoting on grains immediately downstream. Furthermore, he theorized that the amount of grain roll influences the height and length of the grain trajectory; the greater the momentum gained in rolling, the higher and farther it travels before striking the bed. Such would be the saltation of grains without the influence of eddies. When turbulence is strong

enough to produce a significant number of eddies near the bed, the grain trajectories will be altered to conform with the eddy movements.

When water flows over a bed of sand, it exerts forces on the grains which tend to cause the grains to move. The chief forces in the initiation of motion are lift and drag forces, which tend to move the particles, and the weight of the particles (relative to the water), which tends to keep the grains stationary. Critical conditions exist when the flow conditions are such that any small increase in them will result in particle motion. The following discussion will consider the lift as being negligible compared to the other two forces (White, 1940). Although neglecting the lift force in the theoretical development may not have proper justification, it is not neglected in actual measurements. American Society of Civil Engineers (1966) points out that the effect of lift is automatically considered, since it depends on the same variables as drag and since the constants in the resulting theoretical equations are determined experimentally.

Particle motion will begin when the drag force, f_d , equals the resistance of the particle, f_r . f_r is expressed in terms of the particle fall velocity, w .

$$f_d = C_1 (\pi/4) d_m^2 \rho U_*^2 / 2 \quad (2)$$

$$f_r = C_2 (\pi/4) d_m^2 \rho w^2 / 2 \quad (3)$$

Thus,

$$C_2 (\pi/4) d_m^2 \rho w^2 / 2 = C_1 (\pi/4) d_m^2 \rho U_*^2 / 2 \quad (4)$$

where C_1 and C_2 are functions of Re_p and some shape factor of the grains. If the shape factor is neglected,

$$U_* / w = \phi_1 (U_* d_m / \nu) \quad (5)$$

This criterion for ripple formation was developed by Liu (1957) and further studied by Plate (1957). It is essentially a variation of the equation of particle motion developed by Shields (1936). Shields found that he could describe the beginning of particle motion by the equation

$$\tau_0 / g d_m (\rho_s - \rho) = \phi_2 (U_* d_m / \nu) \quad (6)$$

where ρ_s is the particle density. Plots of Eqns. (5) and (6) are given in Figs. 1 a and b, respectively. The extrapolation to the left of $Re_p = 1$ is a suggestion by Shields and not based on data. Note that the Shields diagram is linear in the laminar region, $Re_p < 3$.

According to Liu, ripples cannot form in the region below his curve, and if flow conditions over a rippled bed change to a value in the lower region, the bed will eventually revert to a flat condition.

Brooks (1958) used a recirculating flume with a bed of fine sand to investigate the factors governing the equilibrium rate of sand transport. He found that the use of the mean velocity and depth as independent variables and the slope as the dependent variable led to

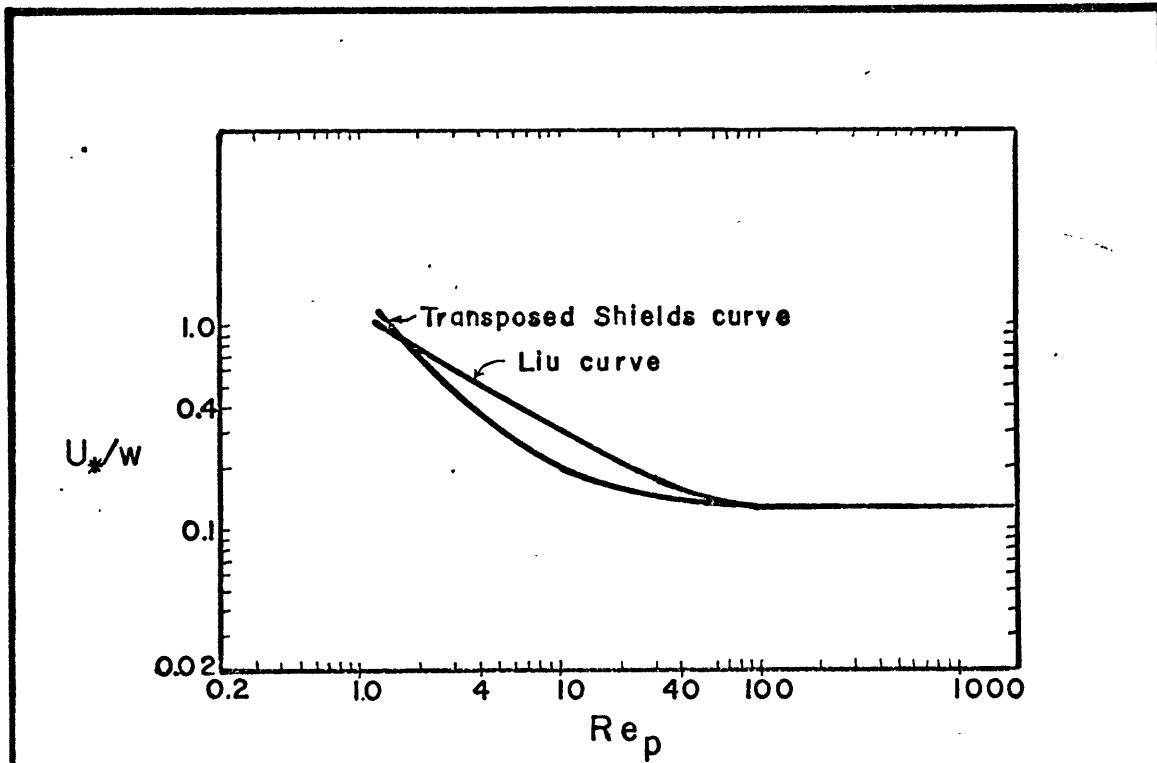


Fig. 1a. - Liu curve with transposed Shields curve

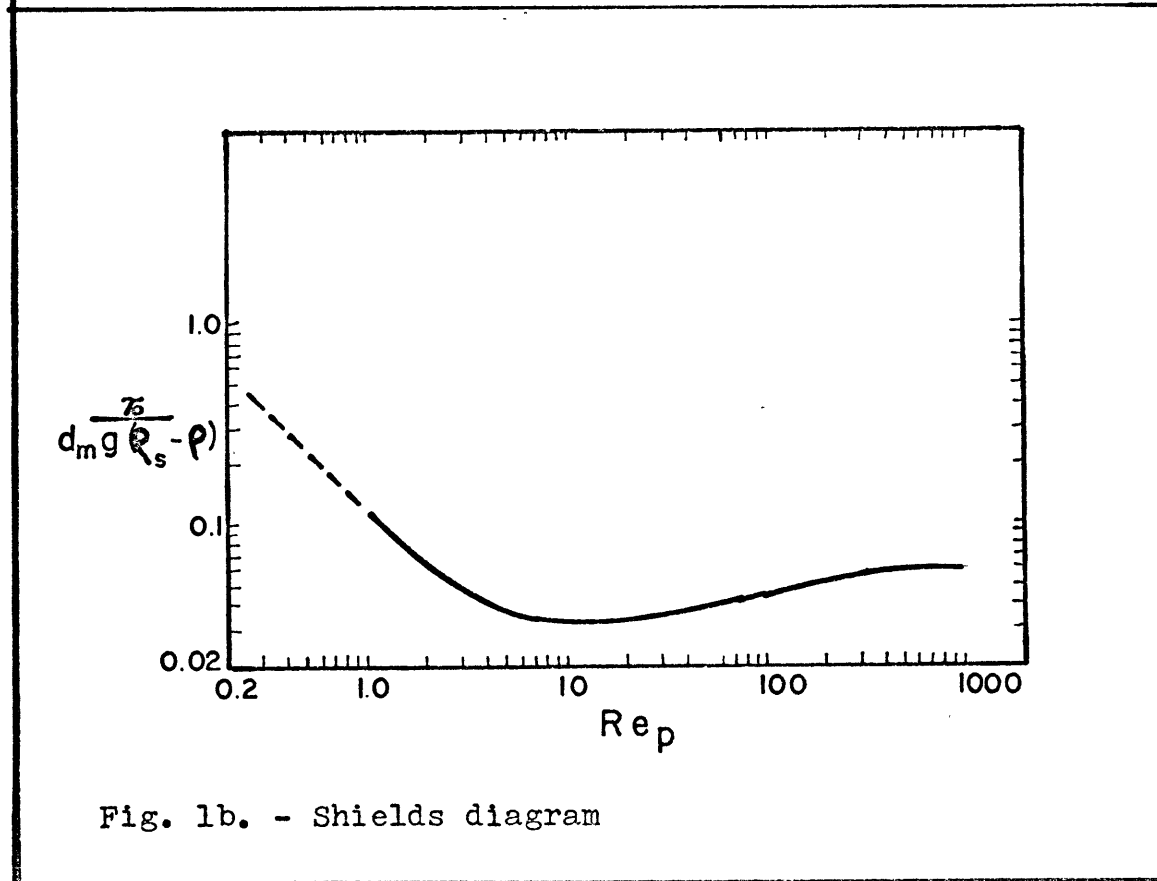


Fig. 1b. - Shields diagram

an orderly relationship between the pertinent variables.

Simons and Richardson (1962) did experiments in a flume 150 ft. long by 8 ft. wide. From this study they developed a relation between the Froude number, Fr , and the kind of bed forms produced (Fig. 2).

$$Fr = U / \sqrt{g y_0} \quad (7)$$

where U is the mean flow velocity.

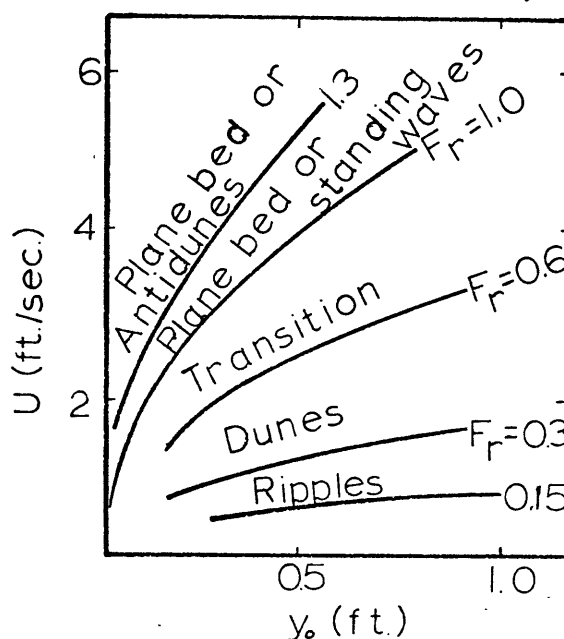


Fig. 2 - Relationship of bed forms to flow regime for fine sand ($d_m = 0.45$ mm)

Kennedy (1963) developed an analytical model to predict the kind of bed form in the different flow regimes. He suggests that initiation of particle motion and ripple formation are synonymous, and that once the critical conditions are reached, the bed is spontaneously deformed into ripples. He also states that any grains piled above the mean level will initiate

ripple growth if the flow is at the critical stage.

Raudkivi (1963) compared a sediment ripple to a negative step in that flow patterns were comparable between the region in the lee of the ripple crest and the region downstream of a negative step. Further, he observed that bed deformation began at some point and gradually spread downstream. The point (or points) of initiation appeared because of a random piling up of the grains. This effect occurred once there was some particle motion. He attributed the piling up to differential particle movement due to: (1) sheltering of grains by other grains, (2) intermittency due to eddies touching the bed, and (3) nonuniform grain sizes.

Once the ripples form, occasional grains are carried over the brink and land five to six crest heights downstream. Such grains either move up the next slope or displace other grains which then move downstream.

The work of Jopling (1965) sheds light on the action of grains as they are carried over the ripple crest. He made a flume study of the formation of a microdelta; a process comparable to the movement of grains over a ripple crest. At low flows, the grains move as bed load, pile up on the upper foreset, and finally slide down the foreset. At higher flows the above occurs, but there are also some grains which are carried into suspension and over the front. These grains are acted on by

two forces: gravity and flow drag. The distance these grains travel as suspended load depends on the relative magnitude of the forces and the height of the crest above the downstream trough. If the grains travel less than some distance downstream (perhaps the five or six crest heights suggested by Raudkivi, 1963) they are actually carried back toward the delta face after settling on the bed. This phenomenon of reverse grain movement is the result of a recirculation eddy in front of the leading foreset; the eddy is caused by flow expansion over the crest. If the strength of the reverse flow is great enough, reverse ripples can actually form immediately downstream of the foreset.

Raichlen and Kennedy (1965) and Sutherland and Hwang (1965) found that the bed friction factors, ripple wave lengths, and dune amplitudes reached over 80% of their equilibrium value in about one-half the development time. The latter authors observed that crests and troughs formed symmetrically at first but then, the troughs changed their vertical dimension faster than did the crests. At the same time, the crests spread out more in the horizontal direction (longitudinally). They attributed these effects to "decapitation" of the crests by the flow.

Sutherland and Hwang (1965) also compared ripple growth from a flat bed and from one "scratched" perpendicular to the flow every few feet. Under the same flow

conditions, they found that the ripples initially grew faster on the scratched bed, but that both obtained the same equilibrium configuration. On the scratched bed ripple growth began at the scratches and propagated downstream, whereas initial formation was random on the unscratched bed.

Rathbun and Guy (1967), studying sediment transport in a small recirculating flume, observed that (1) there was no particle movement on the plane bed before ripple formation, and (2) the mean velocity for cessation of particle movement on the ripple bed was about one-half that at which first movement occurred on the plane bed.

Objective

The objective of this study is threefold:

1. To study ripple propagation downstream of a sediment mound made on the bed for flows above the critical point for particle movement.
2. Repeat (1) for flows below the critical point for particle movement to see if ripples can form under such circumstances.
3. If ripples do sometimes form as in part (2), to develop a technique for predicting the flow conditions and mound geometries necessary for propagation.

It should be noted that Liu (1957) and Kennedy (1963)

suggest that plane-bed grain motion is necessary for ripples to form and propagate even if the bed has irregularities. Rathbun and Guy (1967), on the other hand, observe that grains move on a rippled bed under velocities up to one-half those necessary for plane-bed particle movement.

Acknowledgements

The author wishes to thank Professor John B. Southard for his suggestion of this thesis topic and for his helpful advice throughout the course of the study.

My wife, Janet, deserves special thanks for her encouragement during the course of the work and for the typing of this thesis.

APPARATUS

The apparatus used in this study consisted of a recirculating flume with a bed of fine sand, and an instrument carriage.

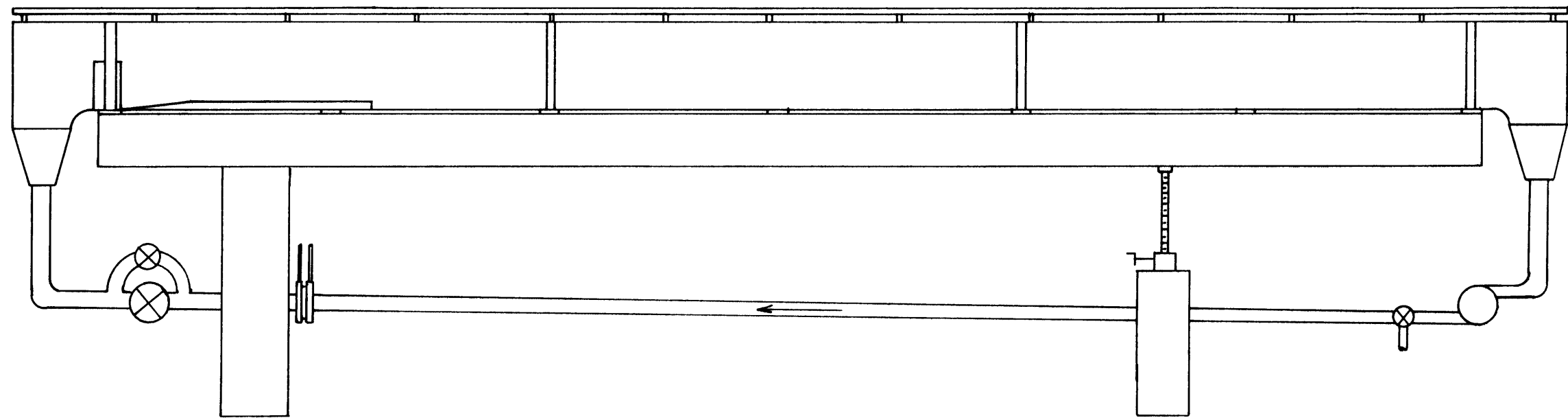
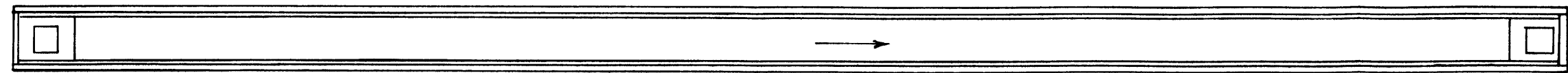
Flume

The flume consisted of a rectangular channel and a return pipe (Fig. 3). The channel was constructed of 3/8 " plexiglas walls and bottom with steel supporting beams and braces. Its inside dimensions were 237" long, 6 1/2" wide, and 13 1/8" deep. A 1 1/2" by 38" false bottom was placed in the upstream end to minimize upstream end effects on the sand bed. A diffuser made of aluminum honeycomb was located immediately upstream of the false bottom.

A pair of steel carriage rails, each offset from the longitudinal center line by 5" and supported by adjustable bolts set in the steel bracing, ran the length of the flume. The level of the rails was adjusted so that they were parallel to a motionless water surface when the flume slope was zero.

Both water and sediment were recirculated from the downstream end of the flume by means of a centrifugal pump through a two-inch galvanized pipe. A centrifugal pump assures uniform flow without pulses for all discharges.

The discharge was controlled by two valves located



RECIRCULATING FLUME

1" = 20"

Figure 3

at the downstream end of the return pipe. Use of valves allowed both fine and coarse control of the discharge.

The discharge was measured with a sharp-edged orifice meter (1.40 " dia.) with flange taps. The orifice was located far enough downstream in the return pipe so that a standard calibration curve could be used (Appendix B). The pressure drop was measured on a water manometer or a mercury manometer, depending on the discharge.

The channel slope was varied by means of a pair of hydraulic jacks at the downstream channel support. The slope could be increased continuously from zero to a maximum value greater than any needed during the study.

Carriage

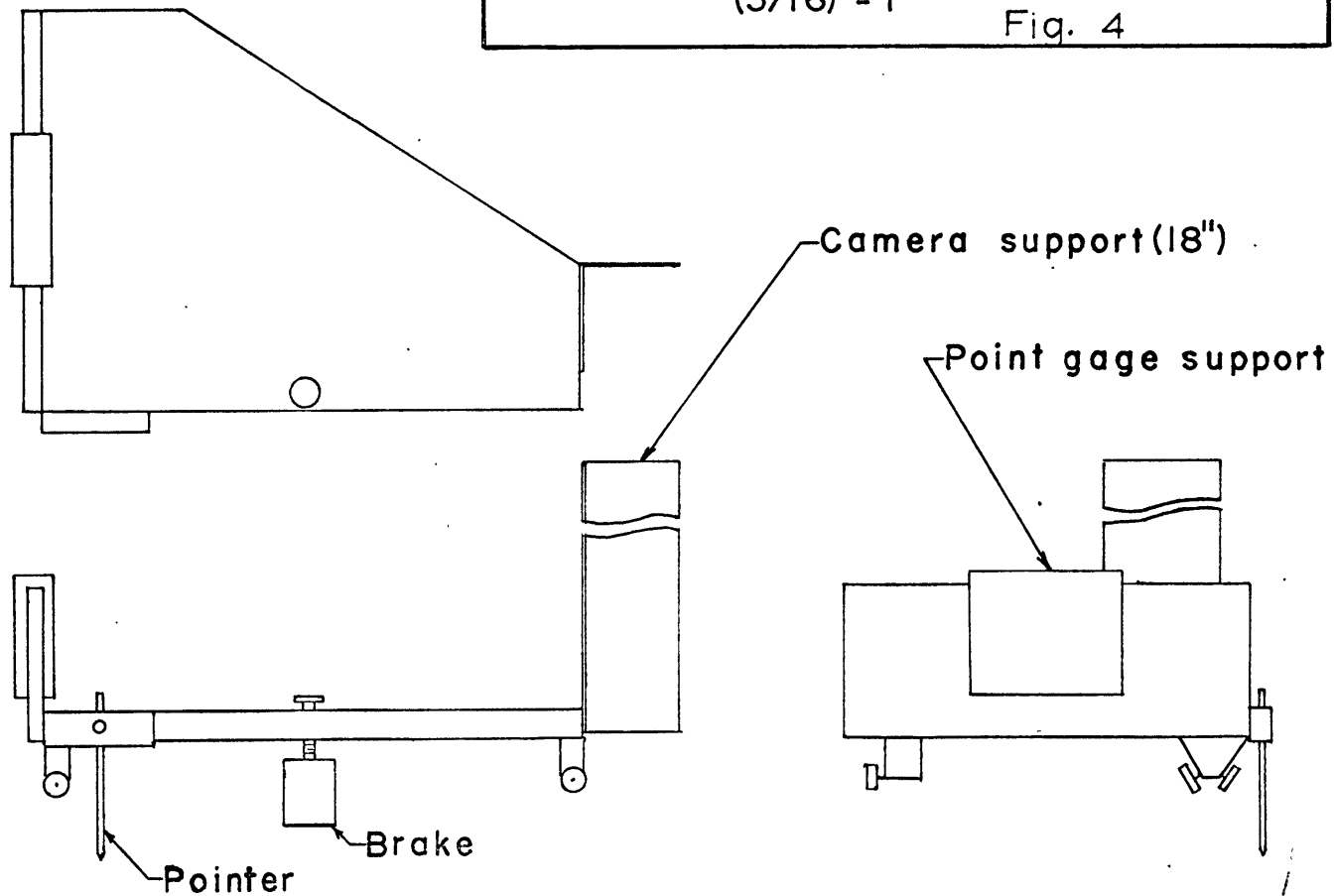
Except for the orifice meter, all measuring devices were mounted on the instrument carriage. The carriage (Fig. 4) was constructed of steel. The point gage support on the carriage front could slide on a flange, allowing depth measurements at any point of the flume. The pointer rode above a meter scale attached to the top of the angle iron supporting the carriage rails. Distance measurements could be read to within 1 mm and could be estimated to 0.1 mm.

A 35 mm Nikkormat camera with a Micro-Nikkor Auto 55 mm, f3.5 lens was used for all pictures. Its height, 18 " above the carriage, permitted a field of approxi-

INSTRUMENT CARRIAGE

(3/16)" = 1"

Fig. 4



mately 30 cm along the flume and completely across it.

When the point gage was removed, a bed leveler could be mounted on the point-gage support. The leveler consisted of two rectangular pieces of 3/8 " plexiglas with a rubber spacer flush with the edges. The leveler could be adjusted to any height and could reproduce bed heights to better than 0.1 mm.

Sand

The same sand was used for all runs. The sand was # 100 crushed quartz sand from the Mystic, Connecticut division of the Ottawa Silica Company. The sand was used as it came from the plant, except that the silica flour was removed by decanting, and the iron filings were removed with a large magnet. Fig. 5 shows a sieve analysis. A photomicrograph of the sand (Fig. 6) shows the grains to be somewhat angular. The statistical parameters of the sand are (Folk, 1961):

$$d_{50} = 0.125 \text{ mm}$$

$$d_m = 0.125 \text{ mm}$$

$$\sigma_I = 0.38 \text{ (well sorted)}$$

$$S_{KI} = +0.1067 \text{ (positively skewed)}$$

$$K_G = 1.29 \text{ (leptokurtic)}$$

$$w_m = 1.43 \text{ cm/sec (based on spherical grains)}$$

The sand was 99.5 + % quartz.

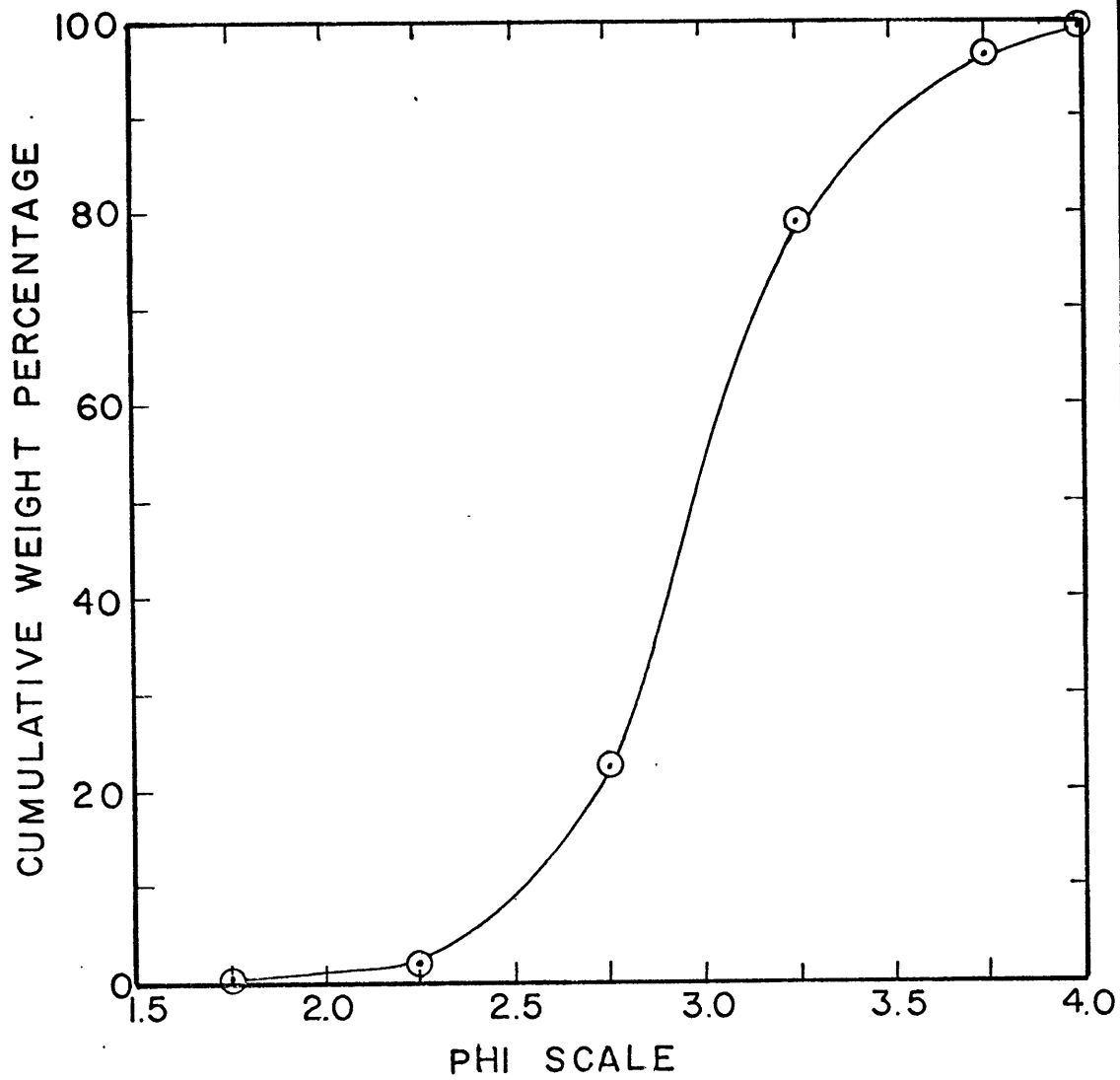


Fig. 5. - Sieve Analysis



Fig. 6 - Photomicrograph of the sand

PROCEDURE

The procedure, the same for all runs, consisted of the following steps:

- (1) Level the bed.
- (2) Set the water depth.
- (3) Adjust the slope.
- (4) Form a sand mound.
- (5) Set the discharge and start the timer.
- (6) Stop the flow to make height and spacing readings and to take pictures.
- (7) Repeat (5) and (6) several times.
- (8) Check the water slope intermittently.

The bed was leveled with the pump off and with several inches of water in the flume. First the bed was stirred up to remove any packing inhomogeneities caused by the ripples of the previous run. Then the bed leveler was lowered to the false bottom, set at that position, and the carriage slowly drawn downstream. Low spots were filled with sand from the downstream end of the bed. This process was repeated until a flat bed of the same height as the false bottom was obtained everywhere in the flume. The bed height was reproducible to the accuracy of the point-gage measurements, 0.01 cm.

The false bottom eliminated the time-consuming process of tapering the upstream end of the bed. The honeycomb diffuser immediately upstream of the false

bottom eliminated any irregularities which might have been introduced by the return pipe. Observation indicated that the combination of the two eliminated any entrance irregularities.

The water depth was set with the pump off. First, water was drained out until the water surface level was slightly below the chosen depth. Then the point-gage was set along the longitudinal center line of the flume and the required depth set on the gage scale. Water was slowly run into the flume until the water surface reached the tip of the point-gage. Finally, the water surface level was read and recorded at the upstream and downstream ends of the flume and the actual depth calculated. In this manner, the actual depth was within 0.01 cm of the desired depth.

The slope was adjusted to approximately uniform flow. The discharge was brought to the desired value and the water surface level measured at several points along the flume centerline. Then the flume was raised or lowered until the water surface was parallel with the rails. Conditions were such that no ripples formed during this time.

Once the slope had been adjusted, the flow was turned off and the water surface allowed to come to rest. At this point, the actual slope of the bed could be calculated by measuring, at both ends of the flume, the

water surface elevation relative to the rails. Thus,

$$S = \Delta H / \Delta x \quad (8)$$

where S is the flume slope for uniform flow, ΔH is the difference in elevation between the two points, and Δx is the distance separating the two points parallel to the carriage rails.

A mound was then manufactured on the bed. The point gage was lowered into the sand along the center-line of the flume and in the upstream part of the bed. The carriage was then drawn downstream a few centimeters and the point gage removed. This left a curved mound as shown in Fig. 7.

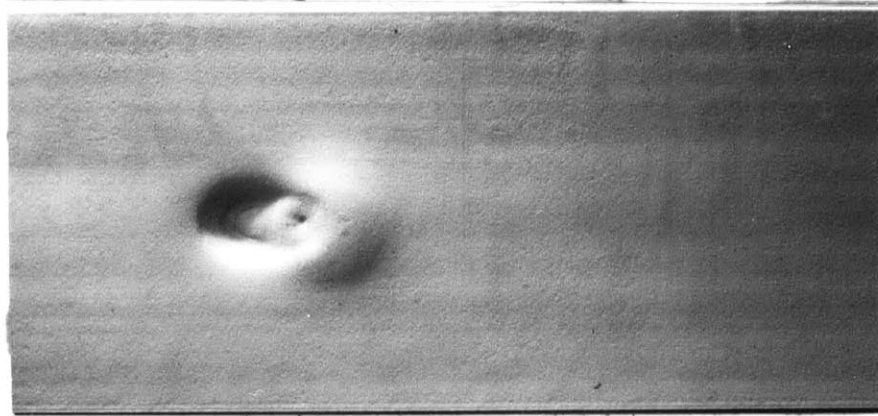


Figure 7 Mound at time zero

The height and position of the crest were then recorded. If a mound of a certain height was required, the above process was repeated until the height was reached. Such heights could be reproduced to 0.01 cm. with little effort.

During the runs to determine the h/y_0 curve, three or four mounds were made on the same bed. In this way uniformity of conditions was assured for runs of a given particle Reynolds number.

During preliminary tests, crests of different geometry were constructed. Although the ripple forms were similar in shape, the growth rates varied somewhat. Therefore, it was decided to make all crests the same shape, and vary only the height.

The discharge was set to the selected value and the timing of the run then started. There was a problem in deciding when to start timing: when grains first began moving or when the desired discharge was reached. The latter method was finally chosen, although this resulted in slight time errors for the higher discharges. The higher discharges were more susceptible to this sort of error, because the discharge had to be turned up slowly to prevent destructive waves in the channel.

At various times the flow was turned off (slowly, to prevent waves) and ripple heights and spacing were recorded. Photographs were usually taken at this time. Time was recorded when the initial reduction in discharge occurred. The run continued until the ripples became too complex to measure, or, in the runs to determine the h/y_0 curve, until it was decided whether or not a crest was going to propagate.

Intermittently, the water surface slope was checked for deviations from uniform flow due to changes in the flow resistance caused by the growth of the bed forms. If necessary, the slope was readjusted until uniform flow was obtained. Insuring uniform flow was the greatest problem encountered, since the shortness of the flume limited the ability to measure depth variations accurately while the run was in progress.

RESULTS

The results of this study are presented in Table 1 and in Figs. 8 - 21 and in Fig. 27. Table 1 lists flow conditions for the runs. Figs. 8 - 17 show crest spacings as a functions of time; they are arranged to correspond to the section of discussion of results (p. 46). One graph (Fig. 18) shows crest height as a function of time, and another (Fig. 27) shows h/y_0 vs. Re_p ; these are placed in the discussion of results (p. 46) for ease of evaluation. The photographs (Figs. 19, 20, and 21) are also placed in the discussion of results (facing p. 49) to permit easy reference while reading the sub-section on crest shape (p. 46).

Intermediate data can be found in Appendix C.

Table 1 - Flow conditions and mound geometries for the runs

(a) $Re_p > Re_{pc}$

Run	U (cm/sec)	y_o (cm)	S ($\times 10^4$)	U_* (cm/sec)	h_o (cm)
1	15.4	4.82	5.96	1.68	0.34
2	15.4	4.82	5.96	1.68	0.34
3	15.4	4.82	5.96	1.68	0.34
4	13.8	4.87	3.85	1.36	0.30
5	13.8	4.87	3.85	1.36	0.39
6	13.8	4.87	3.85	1.36	0.52
7	11.8	3.95	4.71	1.35	0.36
8	15.0	5.15	5.00	1.59	0.46
9	16.7	4.82	6.53	1.76	0.43
10	13.0	3.19	5.95	1.38	0.26

(b) $Re_p < Re_{pc}$

11	10.1	4.70	2.70	1.12	0.47, 0.72 0.95, 1.08
12	10.5	4.76	3.08	1.20	0.09, 0.25 0.38, 0.50 0.76
13	8.7	3.91	1.70	0.81	0.75, 1.15 1.89, 1.53
14	5.3	4.71	0.96	0.67	2.38, 2.88 3.33, 3.81
15	4.4	2.50	1.15	0.53	0.97, 1.50 1.74, 2.00

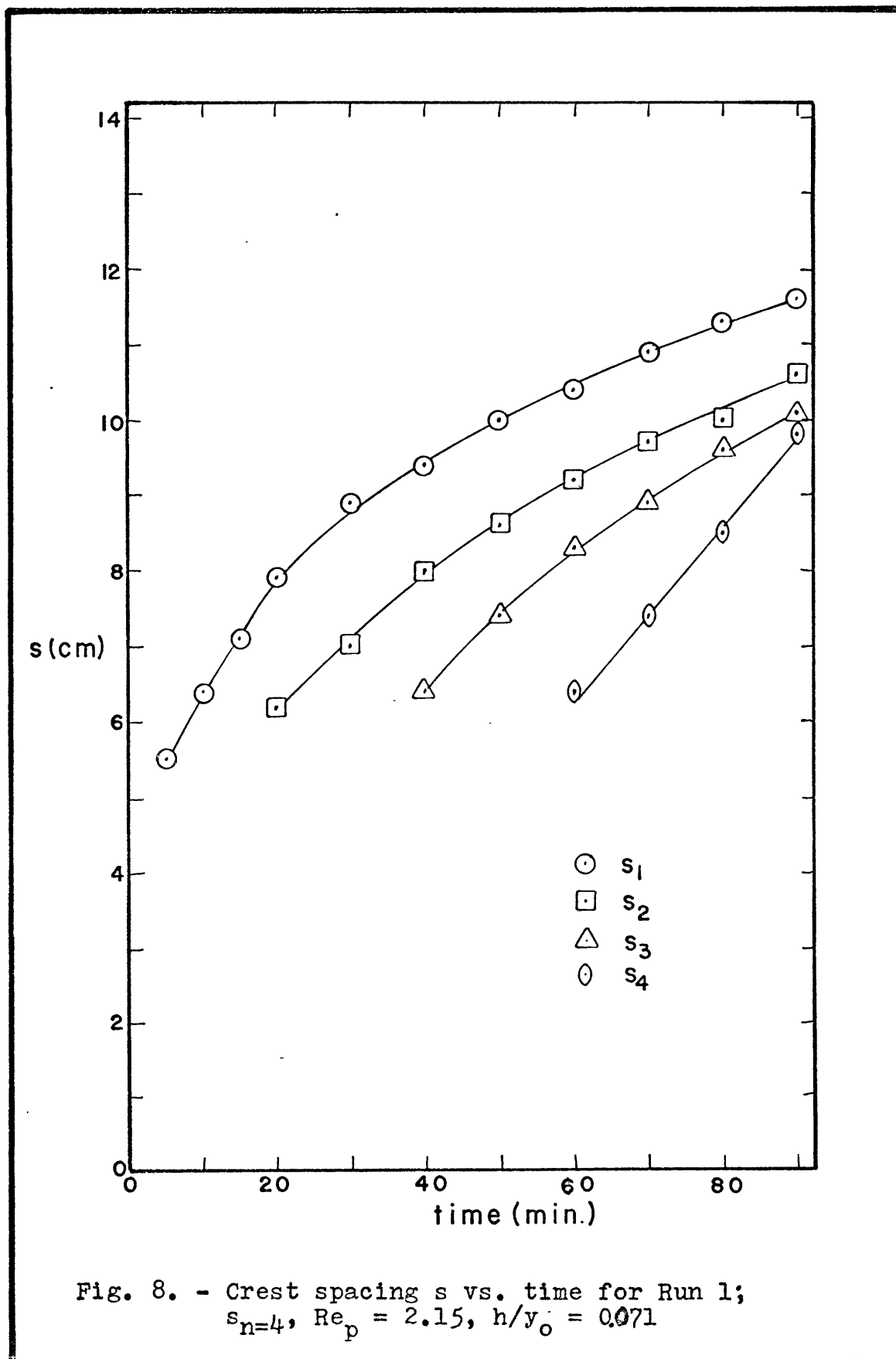


Fig. 8. - Crest spacing s vs. time for Run 1;
 $s_{n=4}$, $Re_p = 2.15$, $h/y_0 = 0.071$

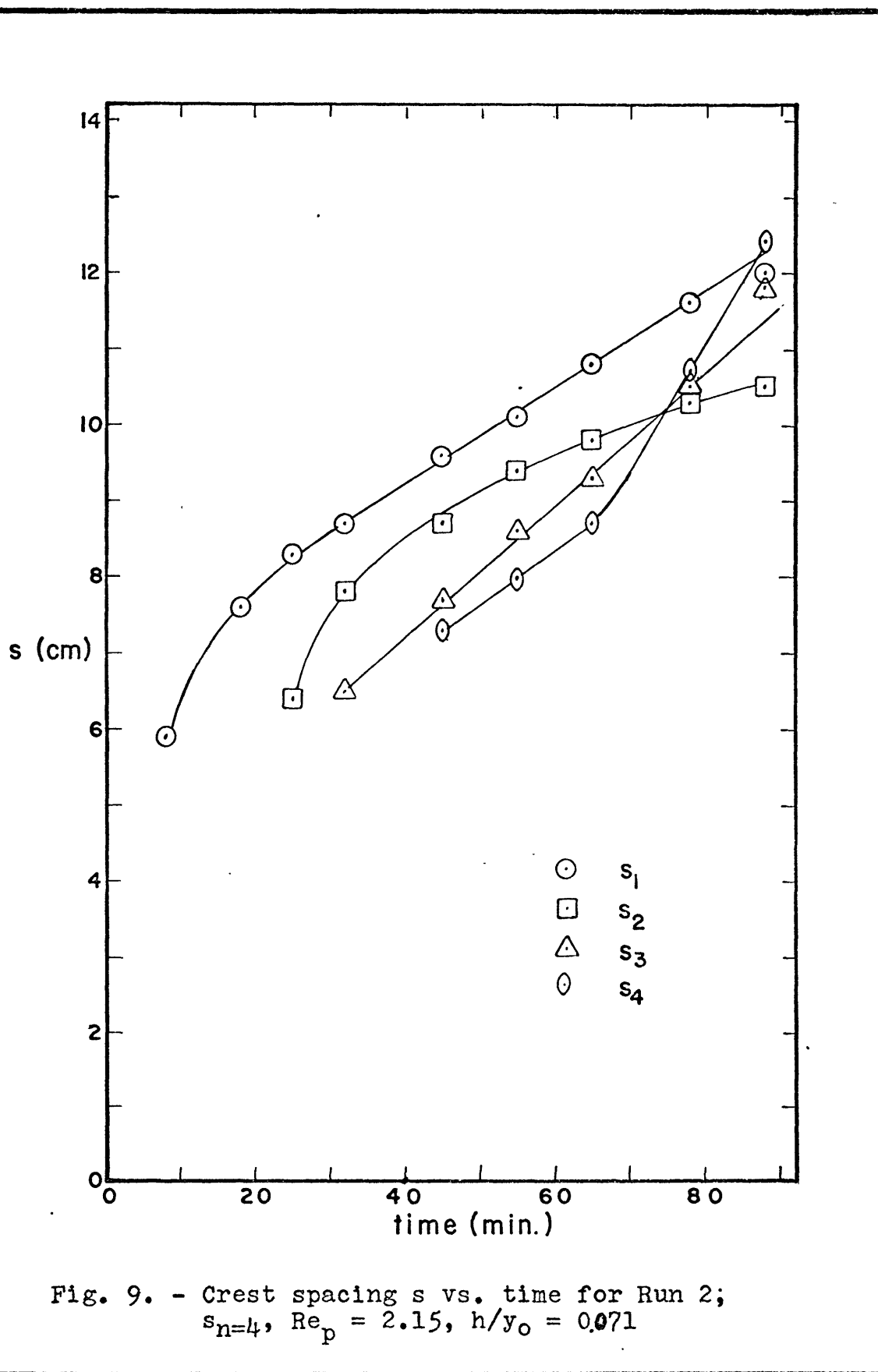


Fig. 9. - Crest spacing s vs. time for Run 2;
 $s_{n=4}$, $Re_p = 2.15$, $h/y_o = 0.071$

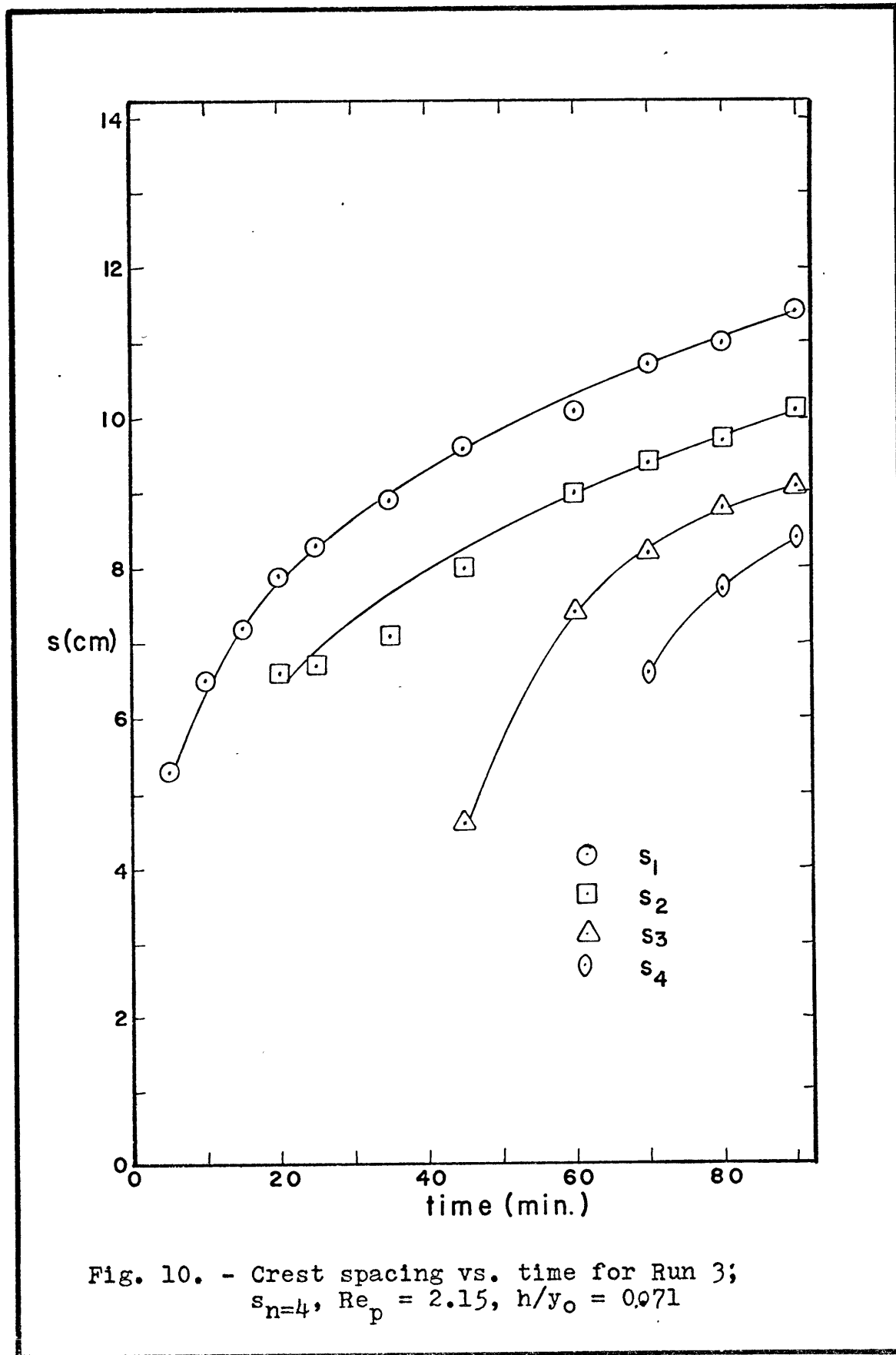
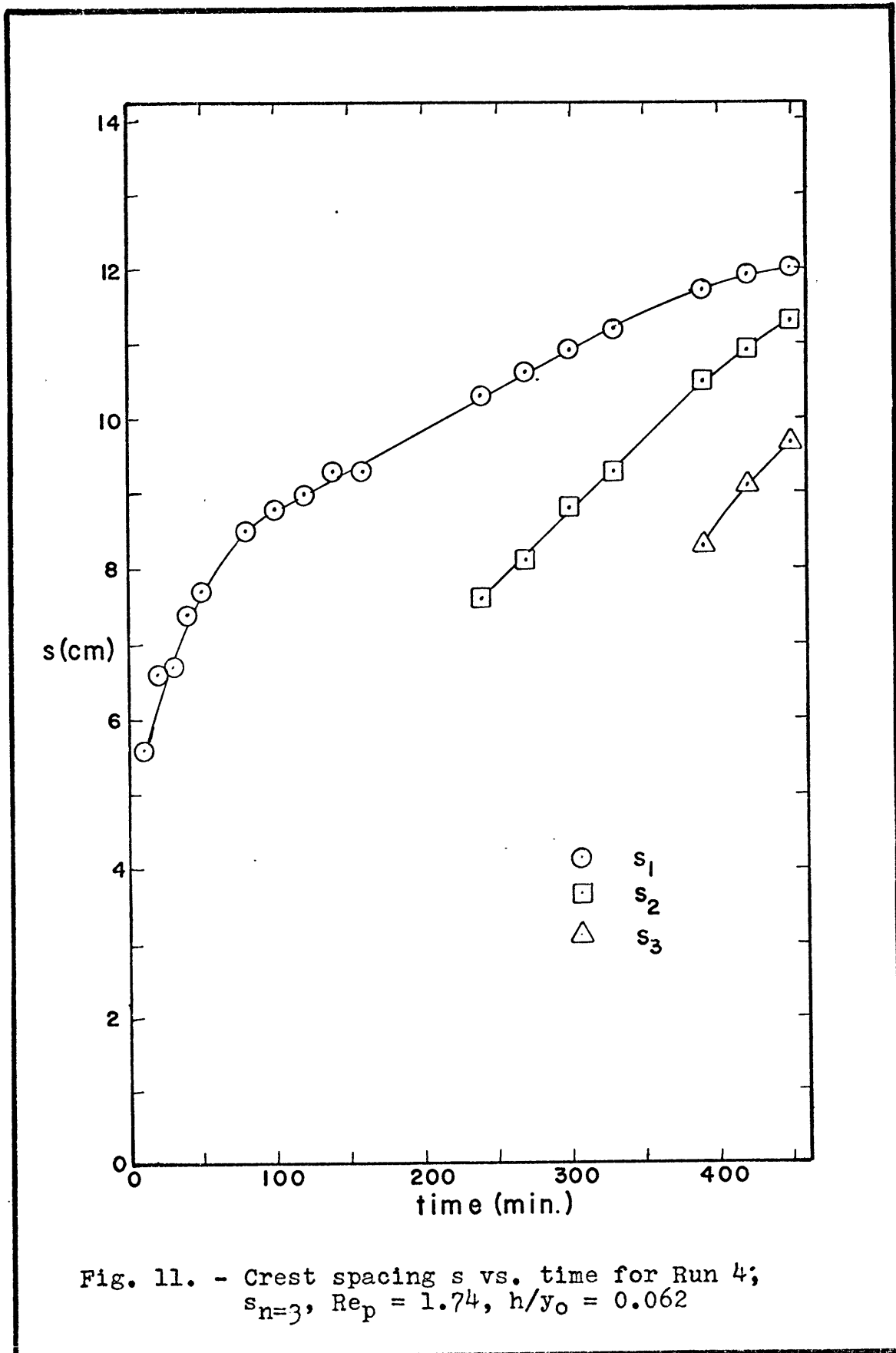
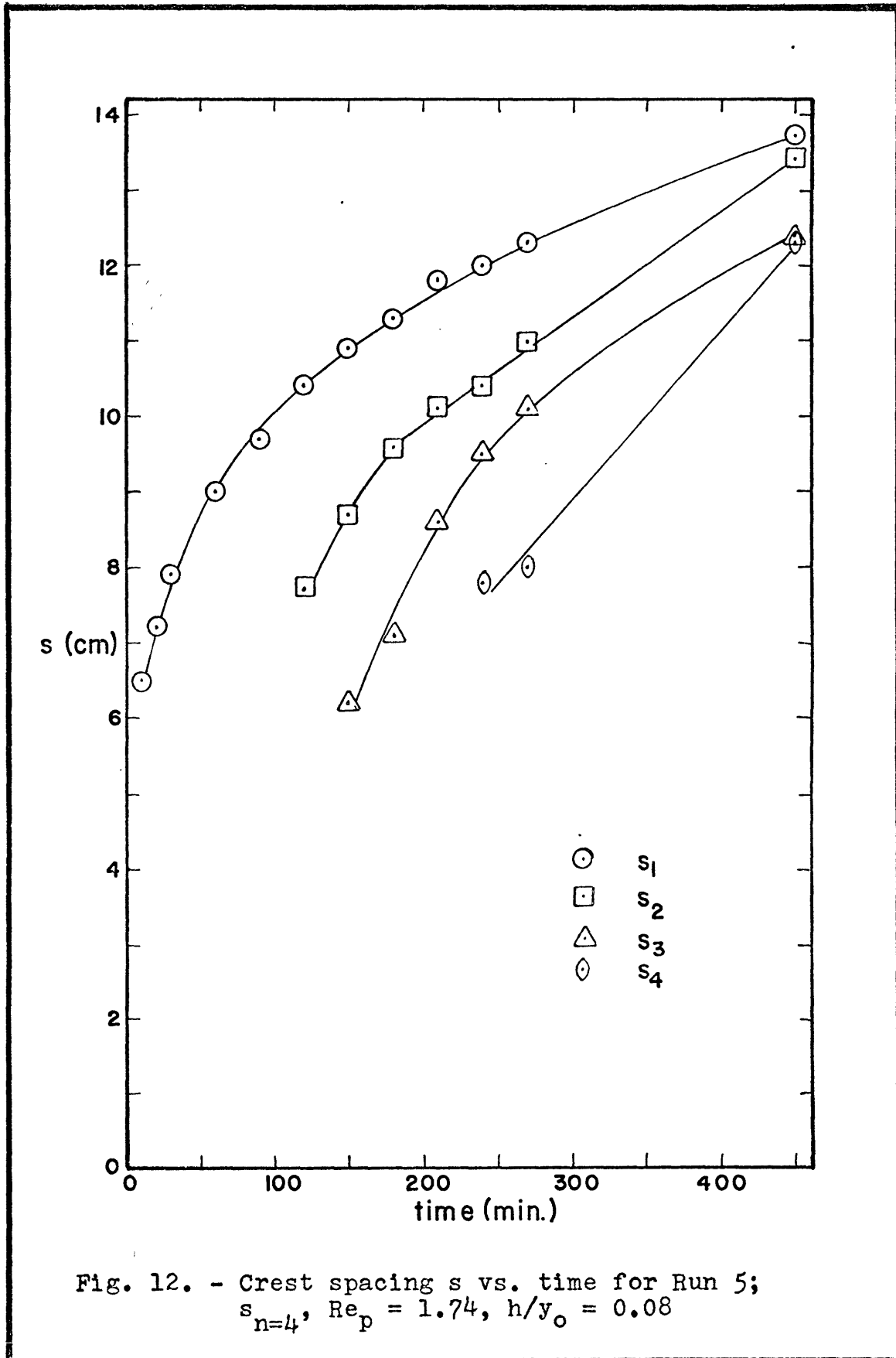
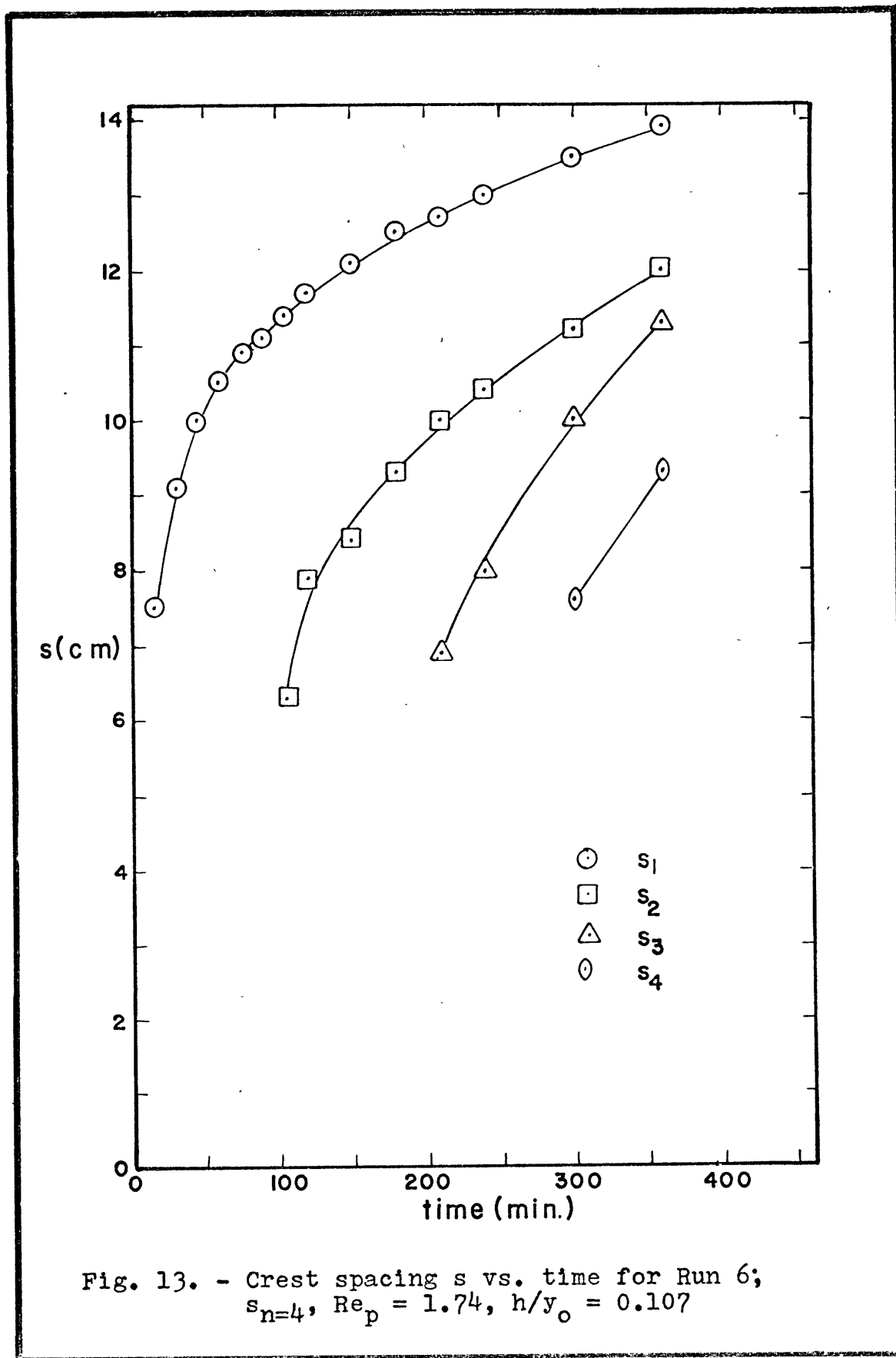


Fig. 10. - Crest spacing vs. time for Run 3;
 $s_{n=4}$, $Re_p = 2.15$, $h/y_0 = 0.071$







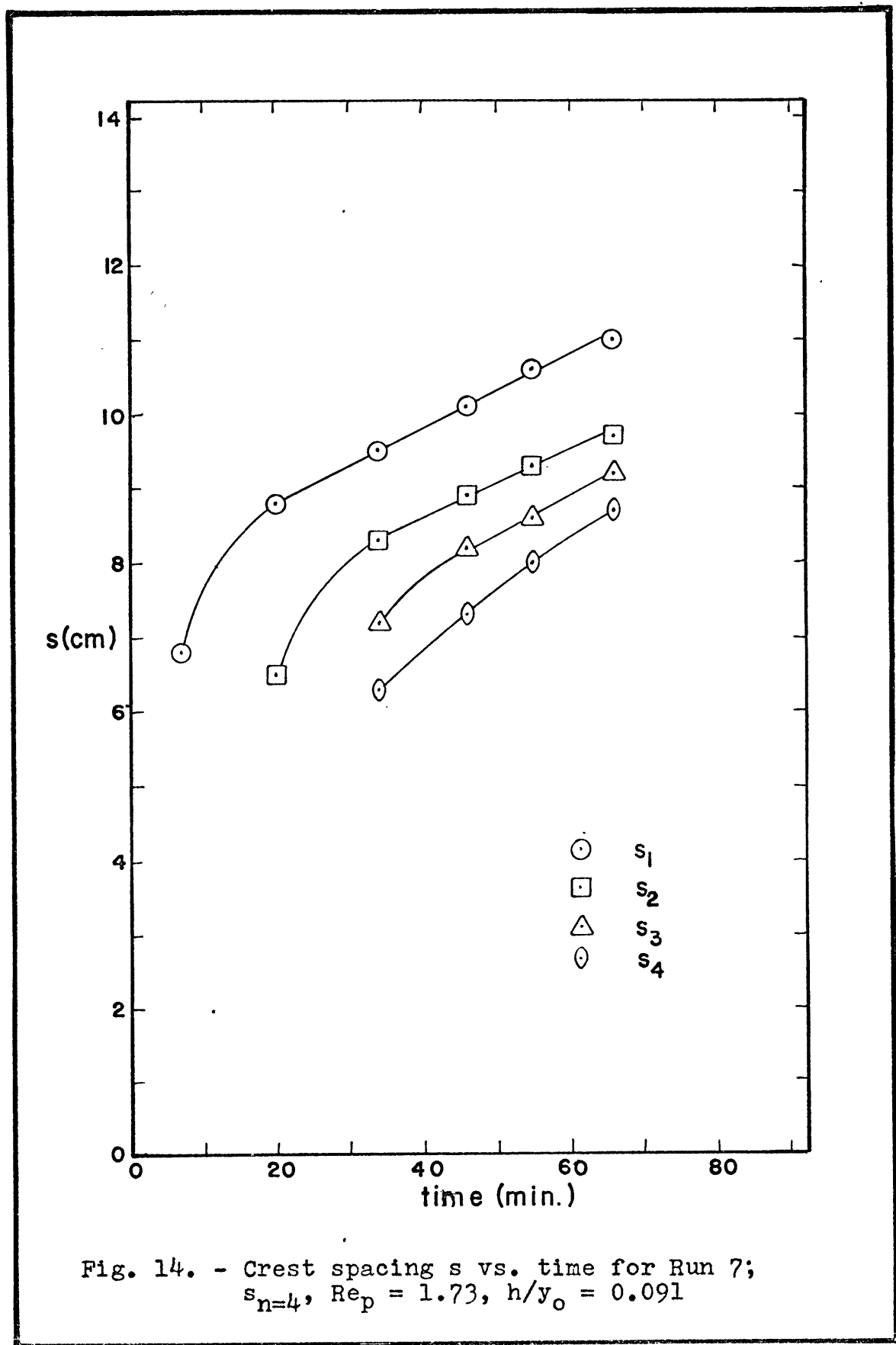
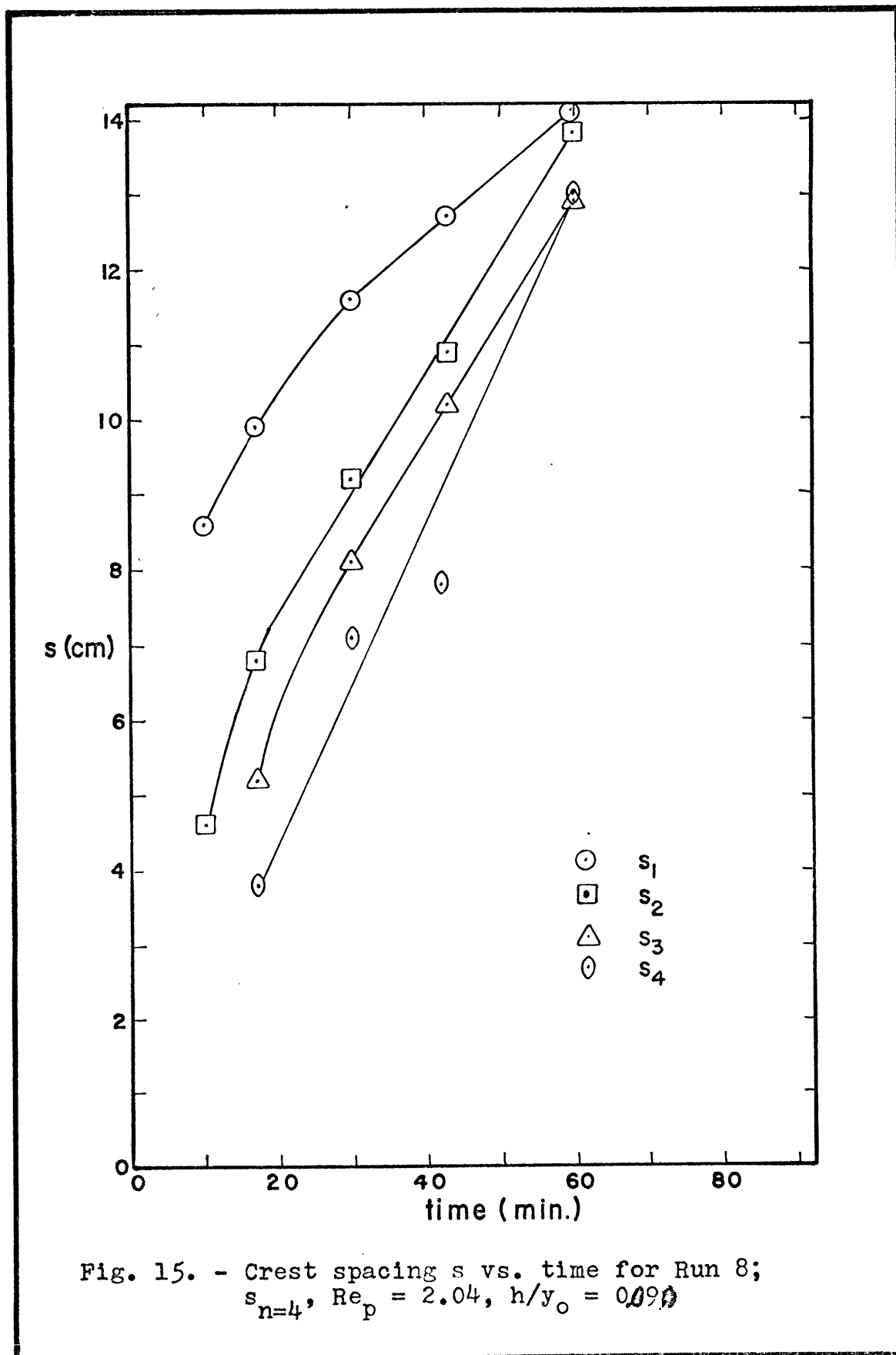
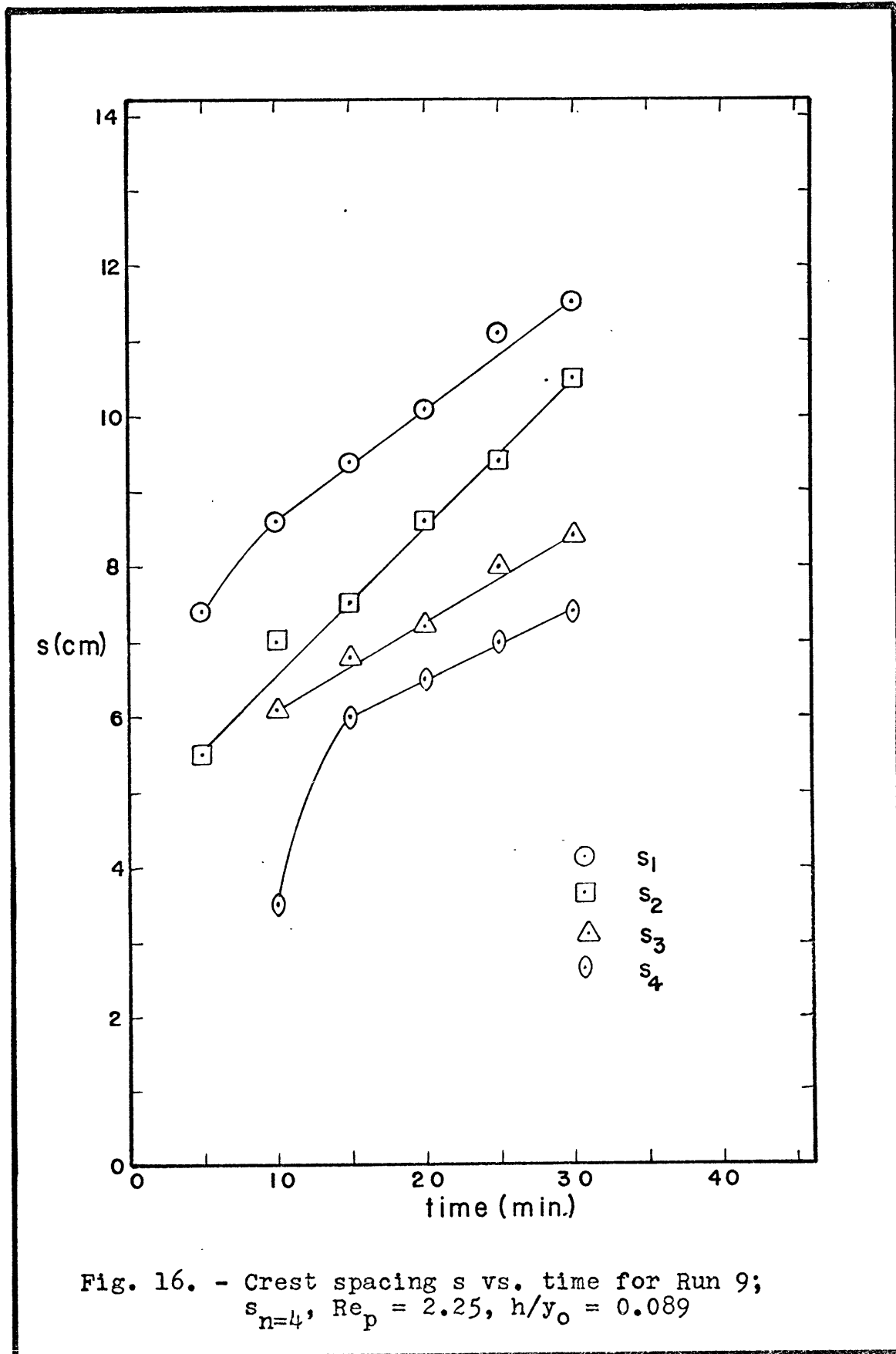
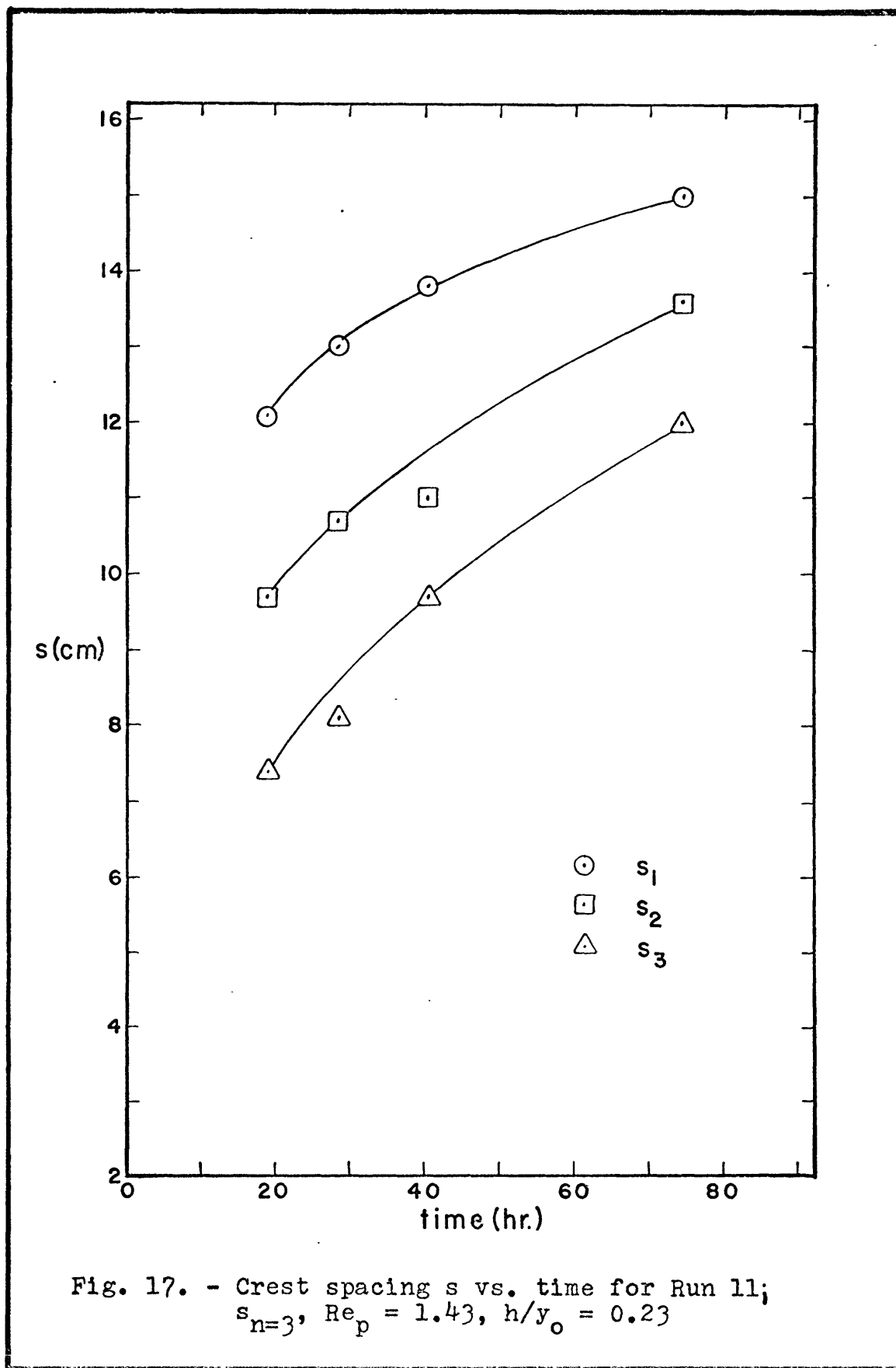


Fig. 14. - Crest spacing s vs. time for Run 7;
 $s_{n=4}$, $Re_p = 1.73$, $h/y_0 = 0.091$







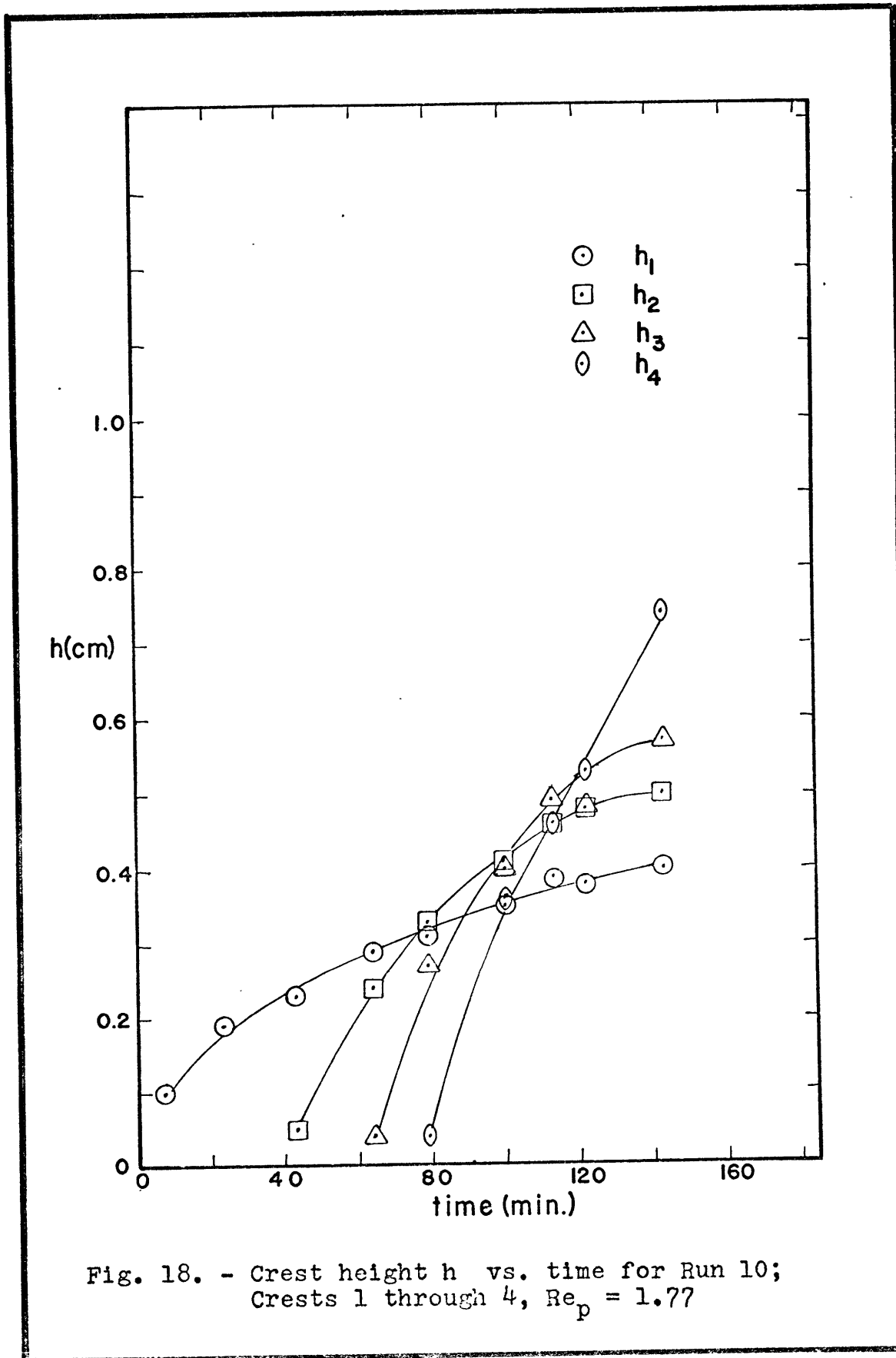


Fig. 18. - Crest height h vs. time for Run 10;
Crests 1 through 4, $Re_p = 1.77$

DISCUSSION OF RESULTS

Crest Shape

Normally, ripples grow across the entire width of the flume and are initially two-dimensional -- except near the flume walls. The ripples formed in this study started with three-dimensional crests and had a width less than the flume width. The difference in shape is a result of the mound, which does not span the flow. Fig. 19 shows photographs of a typical run. Figs. 20 and 21 show other aspects of the shape. A brief discussion of the figures follows.

At time zero a mound is formed with its center on the longitudinal centerline of the flume (see Procedure, p.30). (All subsequent measurements were made along the centerline of the flume). Because of the manner of formation, the mound is curved in shape (Fig. 19a). The mound becomes two-dimensional when the flow starts. At this time there is active grain movement on the stoss slope and in front of the mound.

Within a short time, scour begins just downstream of the mound. The most active areas are downstream of the lateral extremes of the mound; scour marks appear in these two areas (Fig. 19b). Grains move both downstream and toward the flume centerline. Erosion along the centerline is much weaker, with the result that there is a net accumulation of the grains along the centerline.

Soon, the scoured grains begin to organize into the two lobed feature. At first the lobes are separate, each downstream of one of the scoured areas, but eventually they join (Fig. 19b). The intersection point lies on the centerline, and marks the downstream end of a transverse crest. This forms a doubly curved crest symmetrical about the centerline. The lateral extremes tail off until they are indistinguishable from the flat bed. The width of a crest is invariably greater than the width of the preceding crest.

The first crest downstream of the mound retains its lobed shape throughout the run (Fig. 19e), the only changes being that the lobes become angular and that the longitudinal separation between the intersection point and the lobe front decreases. The high point of the crest is not on the front, but just back of the intersection point on the transverse crest. A longitudinal cross-section (Fig. 22) clearly shows the shape of the transverse crest.

After the first crest begins to grow, scour begins anew and a second crest appears (Fig. 19c). In this way the rippled bed grows one crest at a time (Fig. 19d). As more ripples appear, there are variations in ripple shape. The variations can be attributed to two factors: (1) widening of the rippled bed with successive crests, and (2) variations in growth rate between the lobes of a crest.

The widening of the ripples continues until they reach the flume walls. This imparts a "v" shape to the rippled bed when it is viewed in its entirety (Fig. 20). The widening leads to two changes in the ripple geometry: either the lobes stay on the lateral extremes and do not join (Figs. 19e,f), or the number of lobes increases by a factor of two with the addition of another transverse crest per pair of lobes (Figs. 19 e,f). In some cases both effects are seen on the same crest.

When the lobes remain on the extremes of a crest, the interior part of the crest becomes linear. Characteristically, there are no transverse crests in the interior region, and the grains move directly downstream, as in grain movement in two-dimensional ripples. When the extra pairs of lobes form, they usually appear such that the transverse crest (extended) intersects a high point of the previous crest. As before, grain motion is both downstream and toward the transverse crest.

Asymmetry develops when one part of a crest grows faster than the rest. Usually this occurs in such a way that the outside lobes of later-formed crests grow faster than the central, planar portion (Figs. 19 e,f). Sometimes one lobe forms before the other, with the result that symmetry of the lobal pair is destroyed (Fig. 21a). The asymmetry is accentuated in later ripples even though the crest which first showed the asymmetry becomes approximately symmetrical again (Fig. 21b).

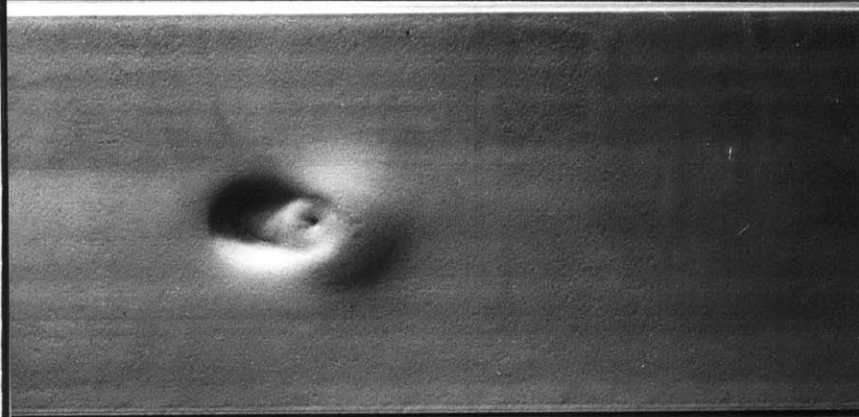


Fig. 19a. - $t = 0$ min

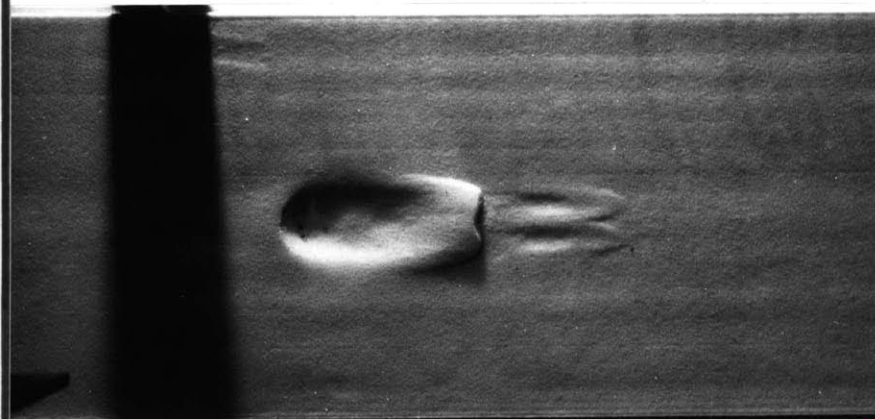


Fig. 19b. - $t = 2$ min

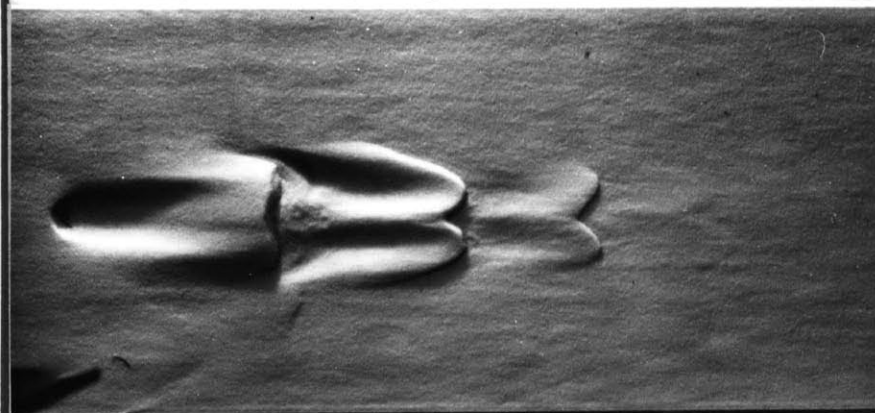


Fig. 19c. - $t = 5$ min

Figs. 19(a-f). - Stages of ripple growth below a mound.
Flow from left to right.

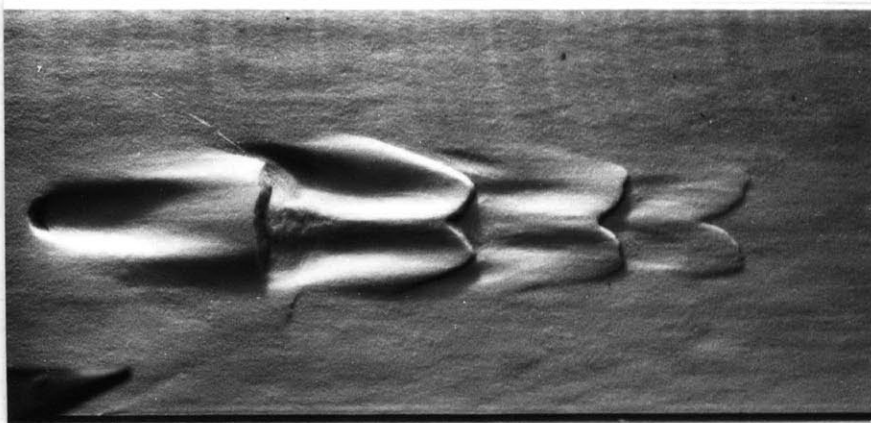


Fig. 19d. - $t = 7$ min

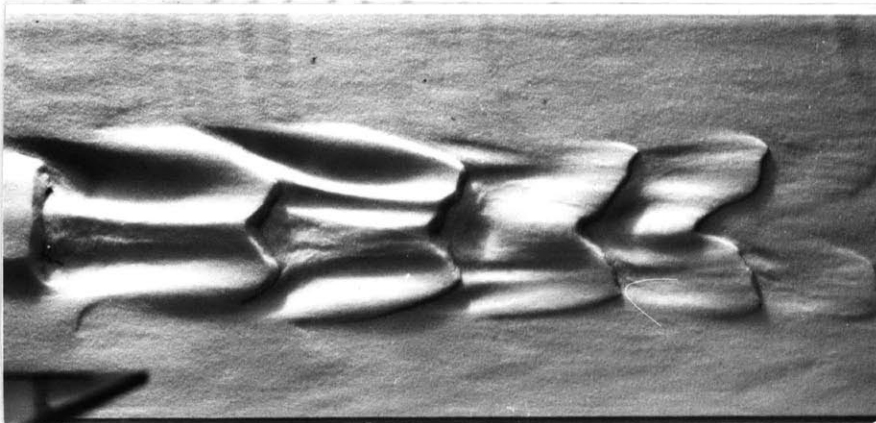


Fig. 19e. - $t = 12.5$ min
(mound at far left)

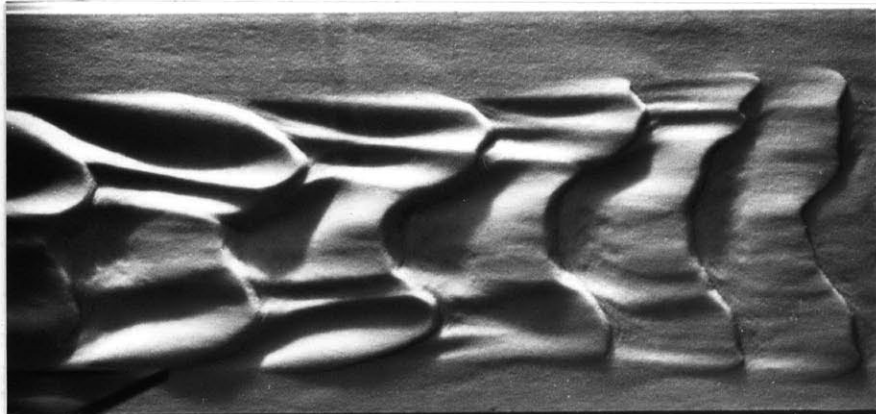


Fig. 19f. - $t = 20$ min (second
formed crest on left)

Run 9 $U = 16.7$ cm/sec, $y_0 = 4.82$ cm

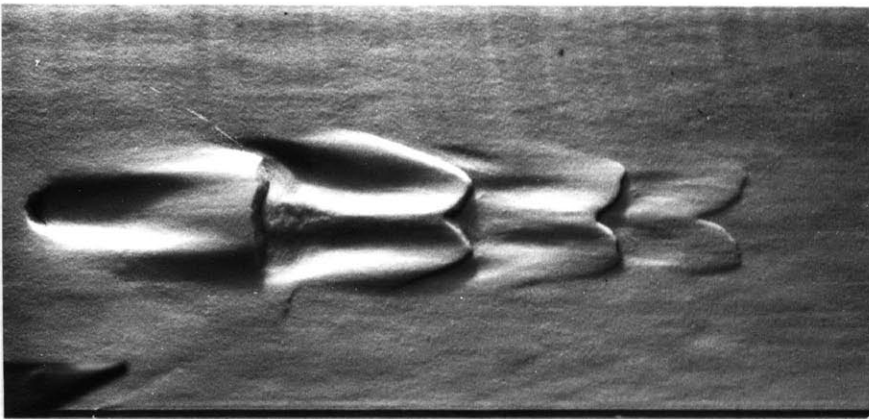


Fig. 19d. - t = 7 min

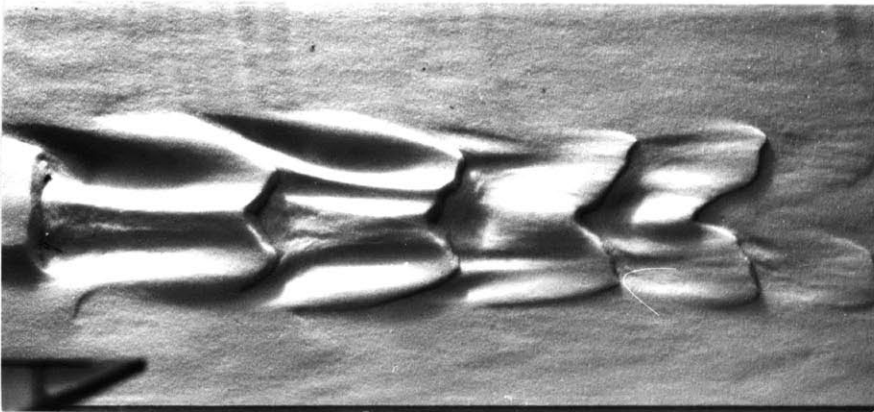


Fig. 19e. - t = 12.5 min
(mound at far left)

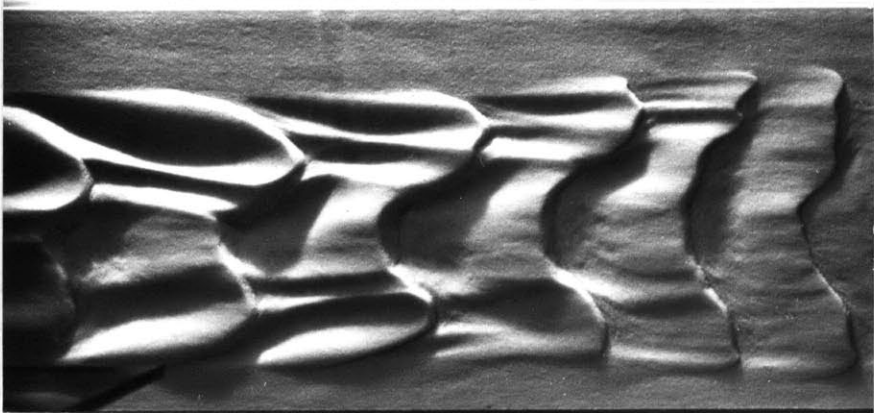


Fig. 19f. - t = 20 min (second
formed crest on left)

Run 9 U = 16.7 cm/sec, $y_0 = 4.82$ cm

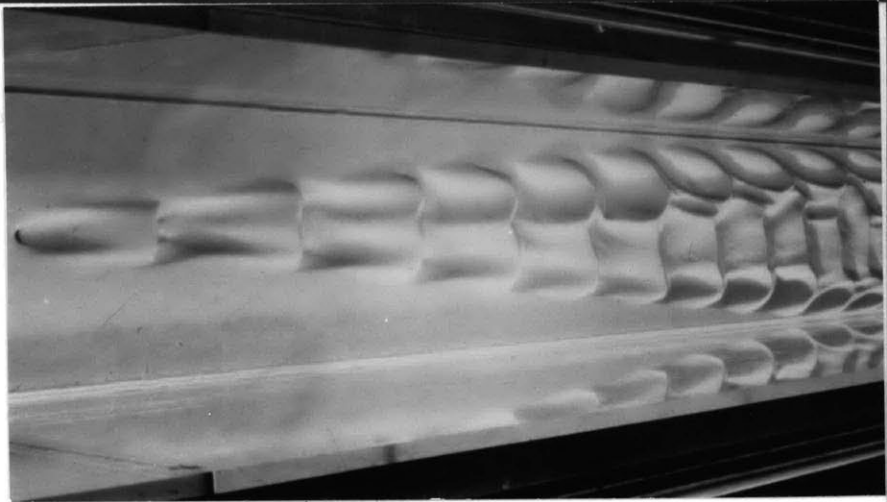


Fig. 20. - Growth of a rippled bed below a mound; typical "V" shape
Run 10, $U = 13.0$, $y_0 = 3.19$

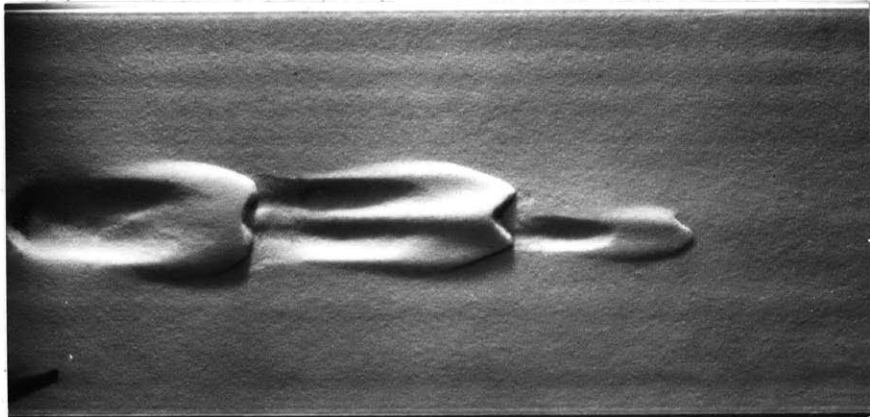


Fig. 21a. - $t = 240$ min

Fig. 21b. - $t = 420$ min

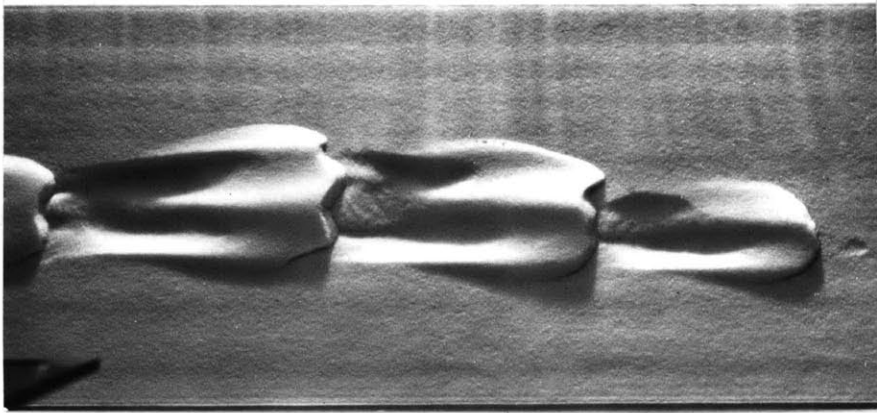
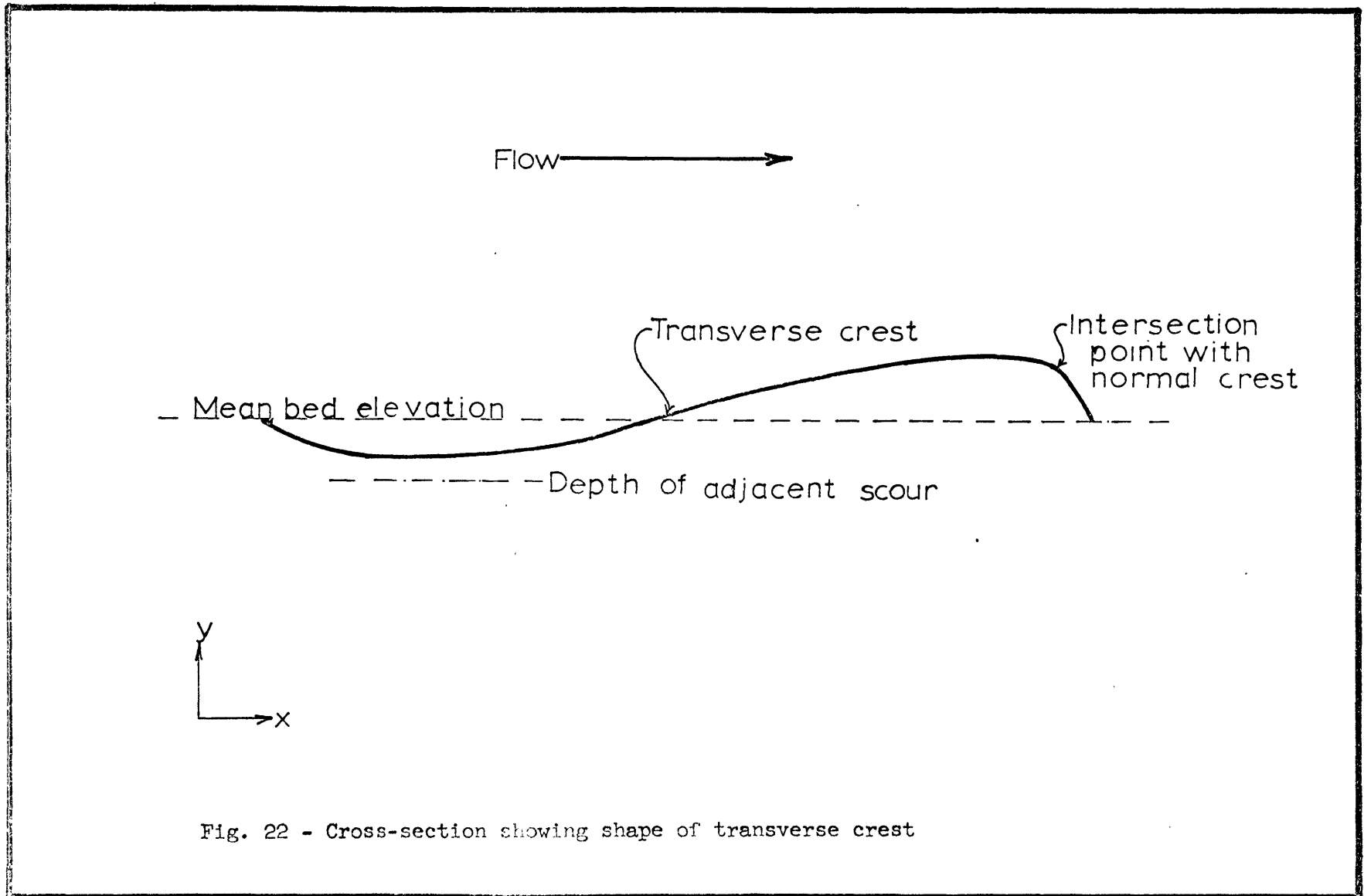


Fig. 21(a,b). - Propagation of asymmetry
Run 4, $U=13.8$, $y_0 = 4.87$



No theory is offered here to explain the shape of the ripples. Instead, a qualitative explanation, based upon the observed grain paths, is offered. When the ripple crest is infinitely wide, the only path for the water is over the crest. After it passes over the crest it forms a zone of separation in the lee of the crest. This phenomenon has been discussed in the Introduction (p. 17).

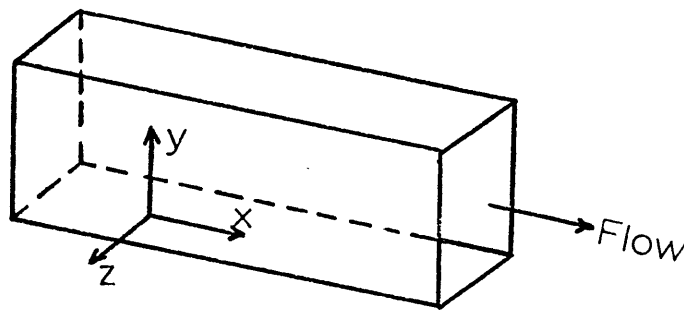


Fig. 23. - Flume coordinate system

When the crests have a finite width, the flow can pass not only over the crest top, but also around the ends of the crest. Consider a coordinate system (Fig. 23) with x , y , and z coordinates as shown. Looking along the x -axis, the mound appears as a hemisphere in the yz plane. When the flow encounters this shape it must not only curve upward (increasing y) but also outward (increasing $|z|$); the relative magnitude depends on where the flow crosses the hemisphere. The downstream result is convergence both downward ($-y$) and inward ($-|z|$), with the flow subsequently impinging on the bed. The consequence is grain movement which is

inward and downstream. Since motion is symmetrical about, and inward toward the centerline, grains will be piled up along it. Thus, lobes with transverse crests will appear downstream of crestal highs, while linear crests form downstream of crests of uniform height.

Ripple Growth; $1.66 < Re_p < 2.50$

The critical particle Reynolds number Re_{pc} is 1.66 for sand with $d_m = 0.125$ mm in 70°F water. The value is obtained by a trial-and-error solution of the Shields diagram as modified by Liu (1957). Given enough time, if $Re_p > Re_{pc}$ ripples will form on a flat bed. For the range of Re_p studied, the time for the appearance of ripples is of the order of hours. Use of a mound speeds ripple formation and permits study of the sequential development of crests without encountering the problems of random appearance.

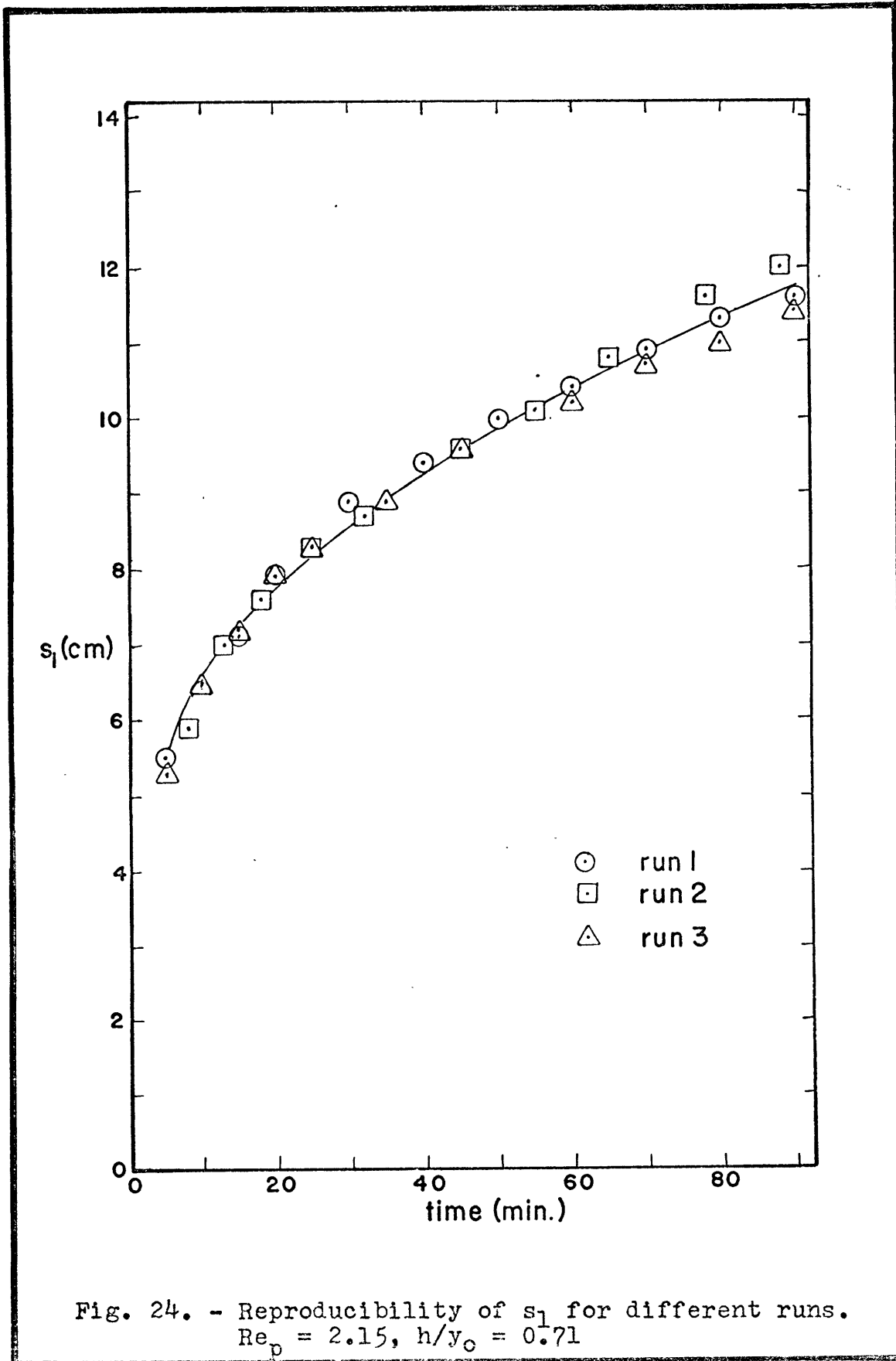
The data have been arranged to illustrate three aspects of ripple development: (1) reproducibility of bed forms under constant flow conditions and ripple geometries, (2) effect of variations in mound height at constant flow conditions, and (3) effect of varying flow conditions on mounds of constant relative height h/y_o .

For ease of discussion, crest spacing will be denoted by s_i , $i = 1, \dots, n$ with s_1 being the space

between the mound and the first crest, s_2 , the mound spacing between the first and second crests, and so on. The expression $s_{n=r}$ designates all of the crest spacings through number r , while s_r designates only the r th spacing.

All the runs show some general growth characteristics. First, the crests always appear in succession; two or more crests never form simultaneously. Second, the rate of ripple growth, in terms of s vs. t for a given i , is initially rapid and then drops off to some limiting value; this limiting constant growth rate is indicated by m_i . In one of the longer runs the growth rate appears to decrease again, such that m_i approaches zero. This is expected because there is an equilibrium ripple wavelength; it was not further investigated. Third, m_i increases with increasing i for a given run. Finally, at some time the height of the i th crest becomes greater than the height of the $(i-1)$ th crest for at least the first few crests (Fig. 18, p. 45).

The flow conditions and mound geometry of run 1 were repeated in runs 2 and 3 to determine the degree of reproducibility of ripple growth. Fig. 24 shows the increase in s_1 for the three runs, while Figs. 25 and 26 show the increase in s_2 and s_3 , respectively. The data for s_1 could easily be fit to a curve. Some deviations appear in the s_2 plot but a curve still fit all



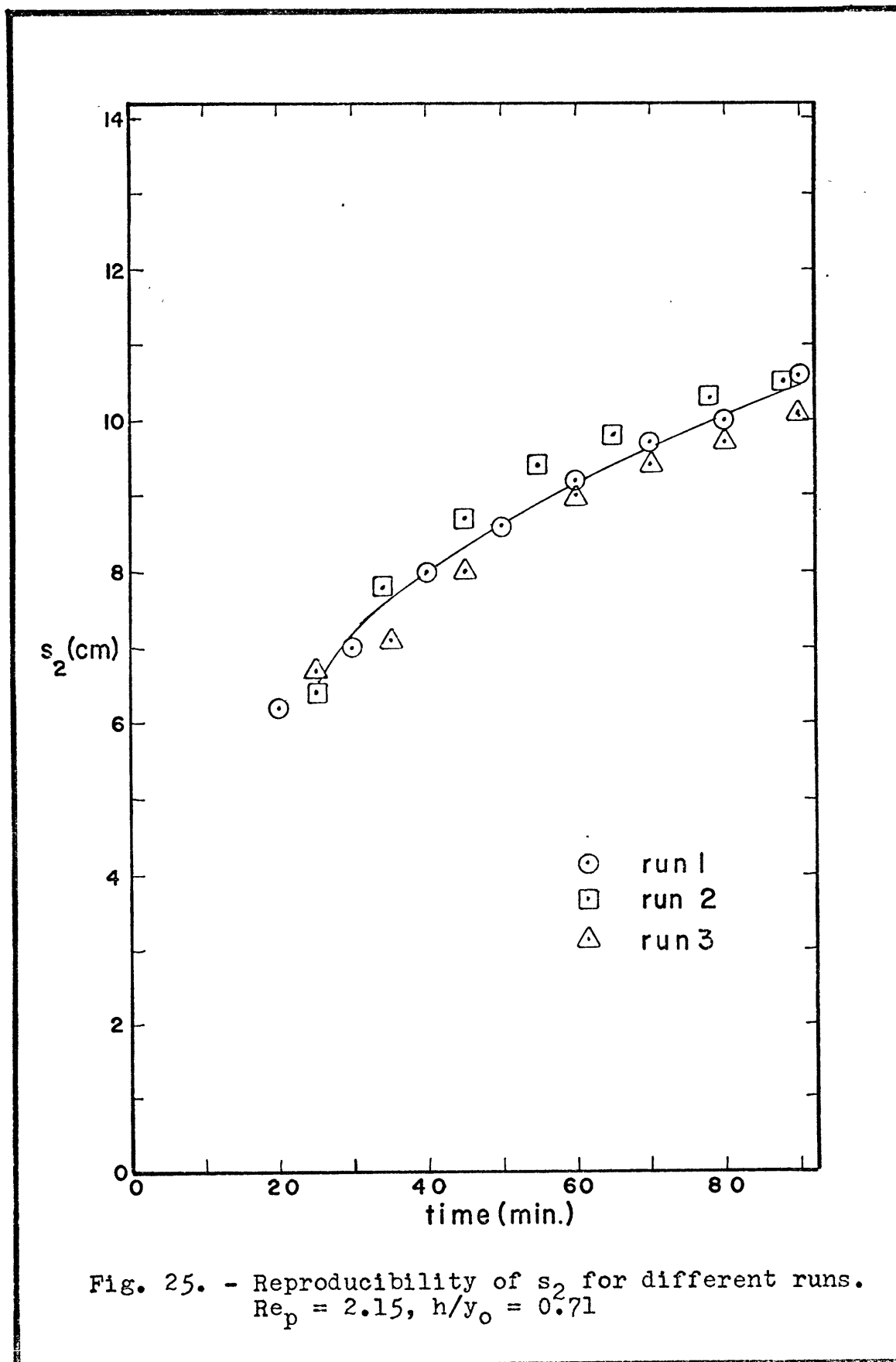


Fig. 25. - Reproducibility of s_2 for different runs.
 $Re_p = 2.15$, $h/y_0 = 0.71$

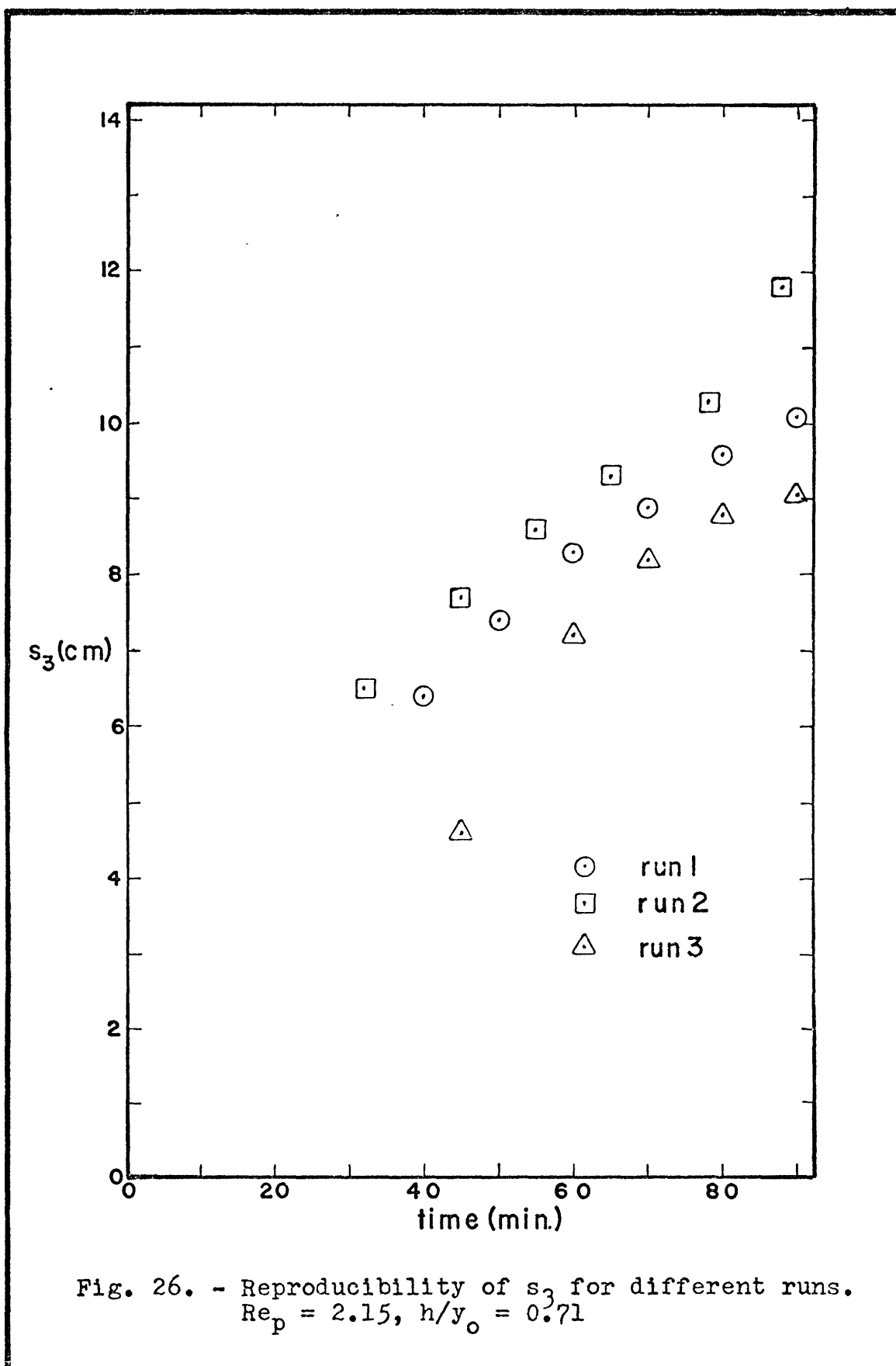


Fig. 26. - Reproducibility of s_3 for different runs.
 $Re_p = 2.15$, $h/y_o = 0.71$

the data. The variations in the data for s_3 are large enough to prevent representation by a curve. Reproducibility is expected to decrease as i increases, because of increased chance for asymmetry, but the plots nevertheless indicate that the ripple propagation is a deterministic process instead of a random one.

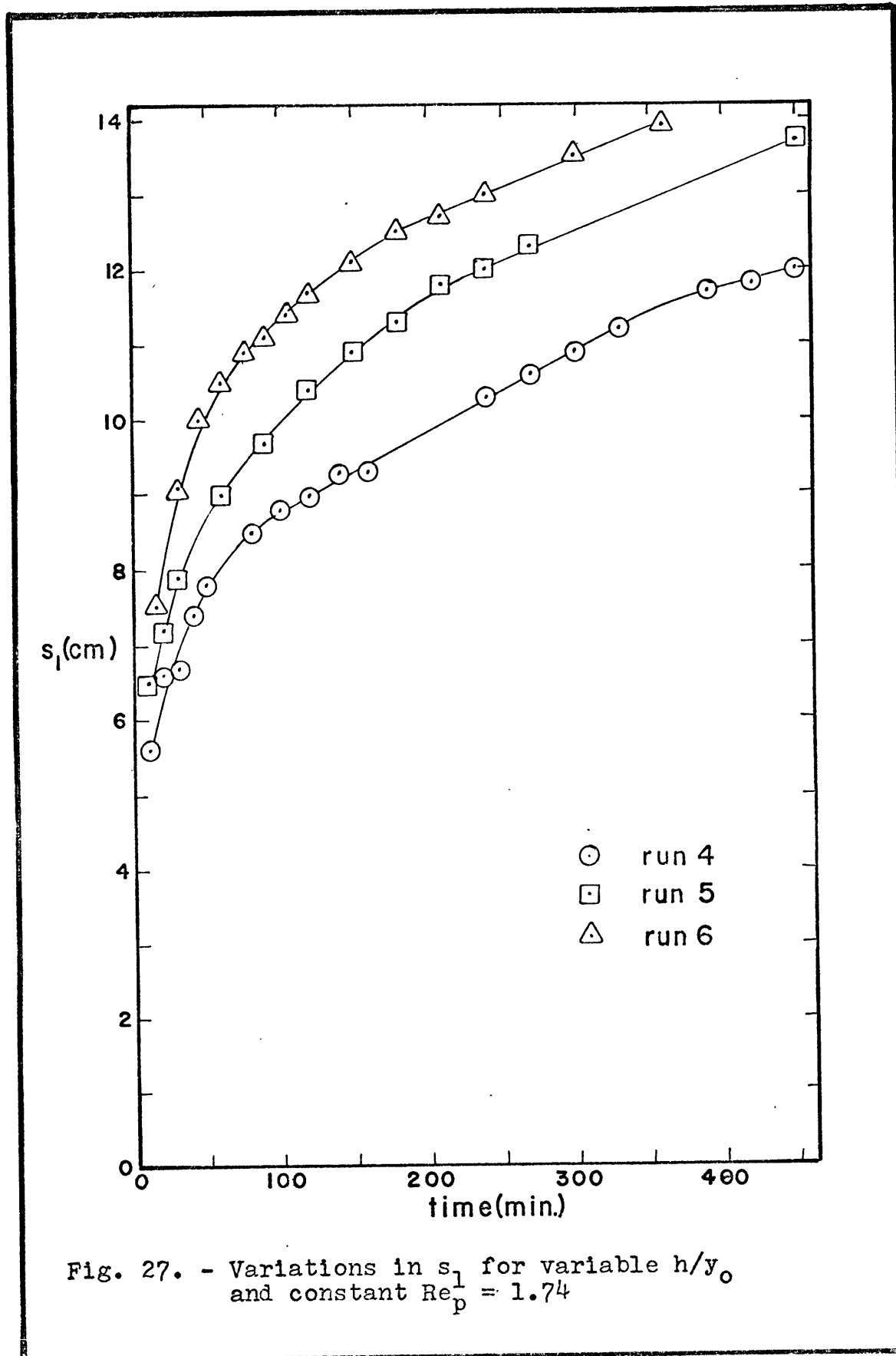
Runs 4, 5, and 6 compare growth rates under constant Re_p and varying h/y_o . The increase in s_1 for the three runs is compared in Fig. 27. Although the three curves have the same slope, they are displaced from each other along the abscissa, with larger h/y_o corresponding to larger s . Since reproducibility of the increase in s_1 has been shown for constant Re_p and h/y_o , the displacement is related to change in h/y_o .

Growth rates change when Re_p is varied and h/y_o is held constant. Table 2 lists $m_{n=4}$ for runs 7, 8, and 9. In general, m increases as Re_p increases for a given s_1 . Exact values of m_3 and m_4 must be held suspect, but the relative values are acceptable to show this Re_p effect.

Table 2

Change in Growth Rate for Variable Re_p
and Constant $h/y_o (=0.9)$

Run	R_{cp}	m_1	m_2	m_3	m_4
7	1.73	0.05	0.045	0.05	0.065
8	2.04	0.09	0.12	0.18	0.25
9	2.25	0.16	0.18	0.11	--



Ripple Growth; $Re_p < Re_{pc}$

For certain values of h/y_0 a rippled bed forms even though there is no flat-bed grain motion. The geometrical and growth characteristics of these ripples are similar to those of ripples formed when $Re_p > Re_{pc}$ (Fig. 17, p. 44). As would be expected, the growth time was of the order of days. There were some mound heights which did not produce a rippled bed (Fig. 28); these mounds invariably caused some initial scour, but the growth eventually ceased. Fig. 28 is divided into three distinct regions and a transition region according to the nature of the ripple propagation.

In Region III a rippled bed forms at all values of h/y_0 , since $Re_p > Re_{pc}$. Of course, the ripples will form sooner if there is a mound, but the purpose of the graph is to show regions of growth and non-growth, and not rate of growth.

In Region II ripples will propagate downstream of a mound even though $Re_p < Re_{pc}$. There is no ripple propagation in Region I. The experimental method prevented an exact determination of the curve separating Regions I and II. Therefore, a region of uncertainty, Region I-II, is shown. This region is bounded by curves through the points of minimum propagation and maximum non-propagation, as determined in this study.

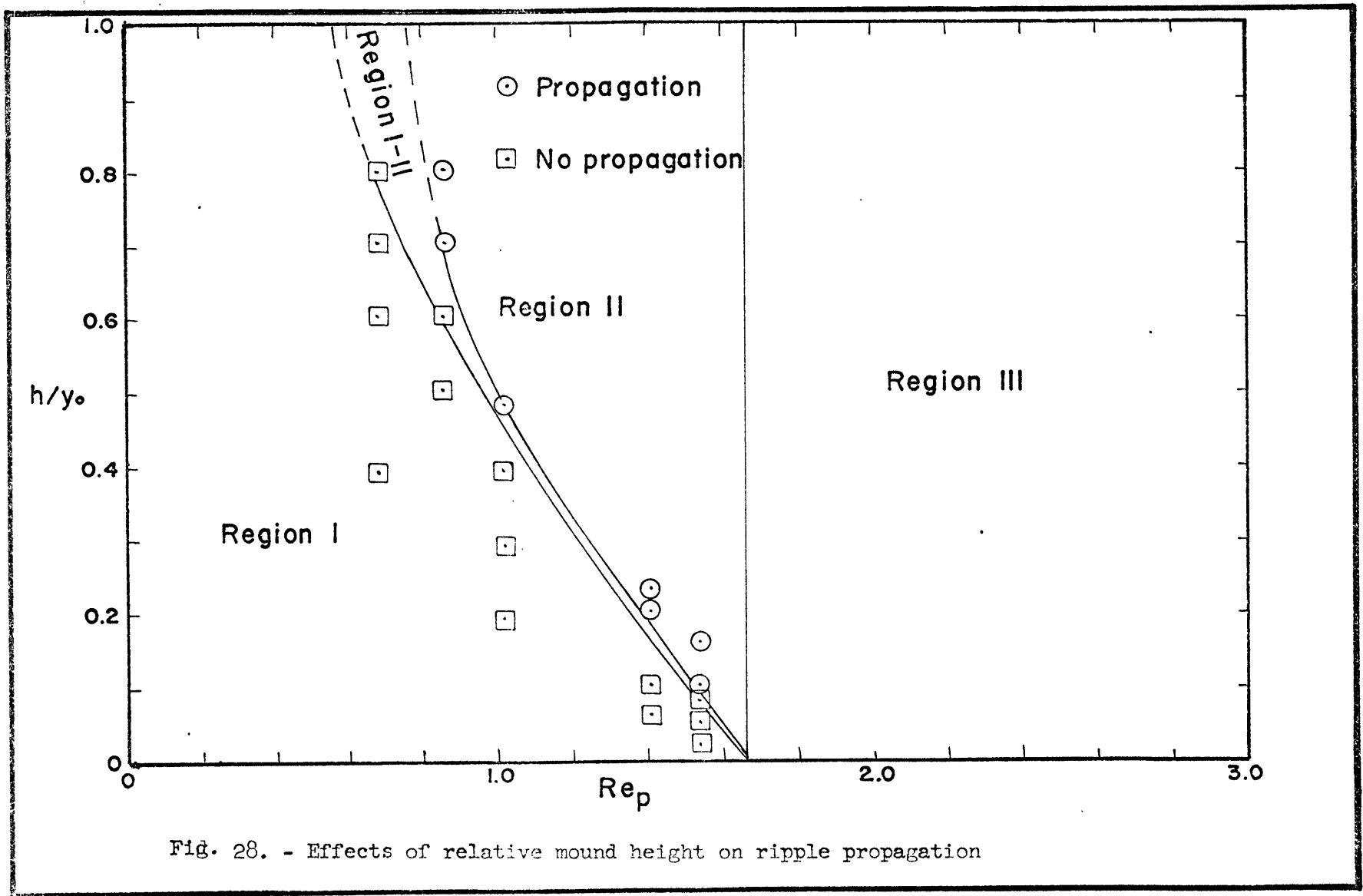


Fig. 28. - Effects of relative mound height on ripple propagation

CONCLUSIONS

- (1) Ripples propagate downstream of a mound for the following conditions:
 - (a) $Re_p > Re_{pc}$ and any h/y_o value.
 - (b) $Re_p < Re_{pc}$ and h/y_o greater than some limiting value.
- (2) Crests forming downstream of a mound of finite width are three-dimensional in shape, with two lobes separated by a transverse crest.
- (3) The scour characteristics downstream of a mound and downstream of crestal highs are the result of the kind of flow expansion. The velocity vector has x, y, and z components, whereas the velocity vector over an infinitely wide crest has only x and y components.
- (4) The spacing between adjacent crests grows in a predictable manner.
- (5) The limiting growth rate (for the times studied) increases as i increases for a given run.
- (6) For a given s_i , the growth rate increases for both increasing Re_p and h/y_o .
- (7) The shortness of the flume prevented accuracy at values of Re_p less than 0.78 because of large inaccuracies in determining the slope at such small slopes.

SUGGESTIONS FOR FUTURE WORK

- (1) The nature of the flow around a crest of finite width should be studied quantitatively.
- (2) Other mound geometries should be studied and compared with the geometry used in this study.
- (3) A longer flume should be used to study the nature of ripple propagation for values of $Re_p < 0.6$.

SUMMARY

Of some interest in the ripple problem is the prediction of the flow conditions necessary to produce a rippled bed; i.e., the critical flow conditions for a given shear velocity and sediment size. Shields (1936) and Liu (1957) experimentally derived curves which predict ripple initiation in terms of the beginning of particle motion, under the main assumption that ripples form when sediment of the mean diameter is in motion on a flat bed. Until recently (Rathbun and Guy, 1967), most authors have believed that a rippled bed would revert to a flat bed if conditions dropped below the critical point.

Although some investigators have observed ripple propagation due to bed irregularities, the writer knows of no detailed studies on this aspect of ripple growth. This study investigates ripple initiation and growth downstream of a mound of bed material. All the work was done in the range $Re_p < 3$, for which ripples propagate more rapidly because of the mound than they grow and propagate from a completely flat bed. The study is extended into the flow regime with no flat-bed particle movement to determine whether a rippled bed would still develop. The possibility of a bed becoming rippled below a mound for such flows has important implications for both geologists and hydraulic engineers. A river bed does not start flat, but has irregularities of various shapes on it. Thus, a rippled bed may not always indi-

cate flow conditions greater than some minimum value, or a channel designed for velocities less than those necessary for flat-bed particle motion may not remain flat.

All the work was done with fine quartz sand ($d_m = 0.125$ mm) in a recirculating flume 20 ft. long, 6.5" wide, and 13" deep. Flow rates were measured with an orifice meter, and spacing and height were measured from a movable carriage. The bed was leveled before each run, and a mound was made on the bed along the flume centerline. Uniform flow was obtained by setting the water depth and flow rate and then adjusting the flume slope, and was maintained by checking the water depth during the run and changing the slope whenever necessary.

At various times during the run, the flow was stopped and crest spacing and crest height measurements were made. Photographs were taken throughout the run.

The data were divided into three parts corresponding to three major aspects of the study. The first part consists of a description of the ripple shape produced downstream of a mound of finite width. The second part is the analysis of ripple growth when the particle Reynolds number is greater than critical. The third part presents the conditions necessary to propagate ripples when the particle Reynolds number is less than critical.

When water flows over a crest of infinite width,

it produces a separation zone in the region in the lee of the crest. At some distance downstream of the crest, the water impinges on the bed and moves sand grains downstream. The grains aggregate at a point further downstream, and another crest begins to form. When the water encounters a mound it flows not only over it but also around it. When the water passes into the lee region of the mound, it has downward and inward velocity components. This causes nonuniform scour on the bed, with two active areas of scour just inside and downstream of the lateral extremes of the mound. The resulting crest is two-lobed with a transverse crest along its longitudinal centerline (Fig. 29).

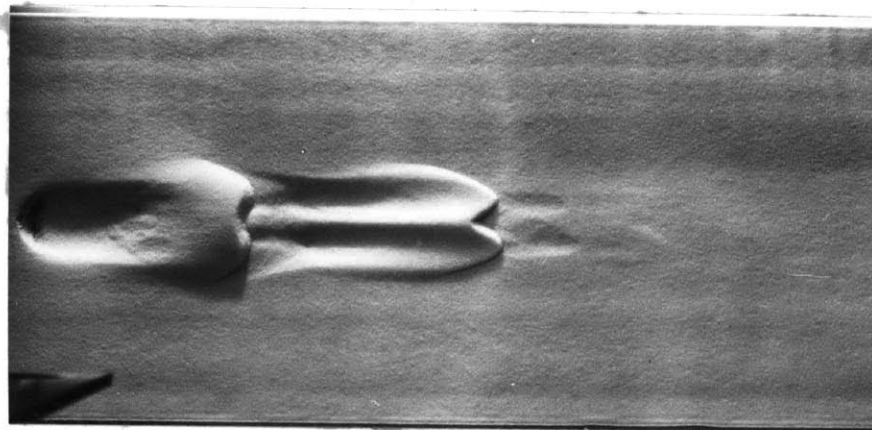


Fig. 29. - Typical two-lobed ripple with transverse crest

The transverse crest forms because the velocity has a component directed inward toward the centerline of the bed in the lee of the mound. This crest shape also appears whenever the upstream crest is of nonuniform height.

Data on growth of these ripples are presented in the form

$$s_i = f(t) \quad (10)$$

where s_i is the crest spacing between successive crests, i and $i-1$ ($i = 0$ for the artificial mound), and t is time. Two trends and the degree of reproducibility are analyzed.

For a given h/y_0 and Re_p the degree of reproducibility decreases with increasing i . The first spacing was reproduced quite well for three runs; the second spacing approximately fit a single curve; the third spacing could not be fit to a curve.

A plot of s vs. t for a given i shows a growth that is initially rapid, but soon decreases to a rate which remains linear over the rest of the run (Fig. 30).

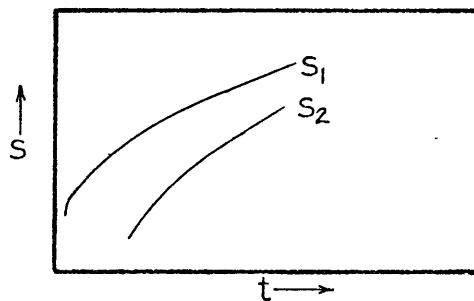


Fig. 30. - Growth of crest spacing s with time. For a given run m_i , the limiting slope of the curve, increases slightly as i increases. For runs in which Re_p was held constant and h/y_0 was varied, the curves for $i = 1$ have the same slopes but are displaced up the s_i axis with increasing h/y_0 . For runs in which h/y_0 was held constant and Re_p was varied, the m_i increases

with increasing Re_p for a given i .

When h/y_0 is greater than some limiting value, a rippled bed forms downstream of the mound even though there is no flat-bed particle movement. This seemingly contradicts the statements of several authors, but perhaps they considered only h/y_0 values less than the limiting value. Fig. 31 shows the limiting curve for ripple propagation. There is some uncertainty in the exact position of the curve because of the low flows involved, but this uncertainty is relatively minor.

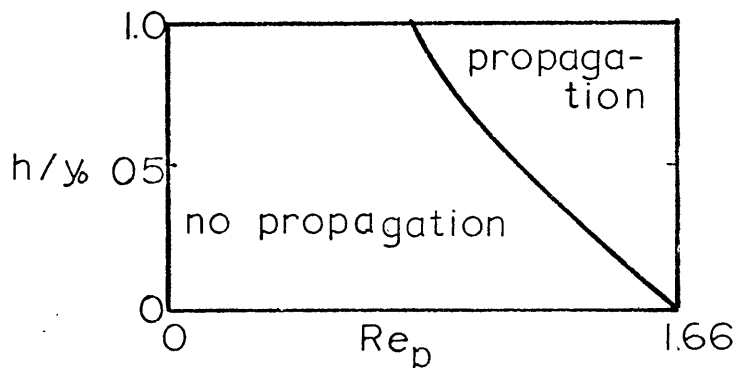


Fig. 31. - Regions of ripple propagation
 $Re_p = 1.66$ is the critical Re_p for sand grains of the mean diameter used in this study (Liu, 1957).

Quantitative work should be done on the patterns of flow and scour downstream of both a mound and high points of a crest. A longer and wider flume would permit study at values of Re_p below 0.78, the lowest value for this study. Work should be done using mounds with other shapes to ascertain the importance of mound shape in ripple propagation.

APPENDIX A

Notation

b	flume width
C_1, C_2	shape factor
d_{50}	median grain size
d_m	mean grain size
Fr	Froude Number
f_o	drag force on a particle
f_r	resistance force of a particle
g	acceleration due to gravity
H	water level reading on point gage
h	mound height
K_G	Graphic Kurtosis
k_s	hypothetical roughness elevation
m_i	limiting value of s_i vs. t curve
R	channel hydraulic radius
R_b	bed hydraulic radius
Re_p	particle Reynolds Number
Re_{pc}	value of Re_p necessary to just move grains of d_m
S	Energy slope = bed slope for uniform flow
S_{KI}	Inclusive Graphic Skewness
s_i	crest spacing between i th and $(i-1)$ th crests
t	time
U	mean velocity

U_*	shear velocity
w	particle fall velocity
w_m	fall velocity of grains of d_m
x	longitudinal flume coordinate
y	vertical flume coordinate
y_0	normal water depth
z	transverse flume coordinate
δ	thickness of laminar sublayer
μ	absolute viscosity
ν	kinematic viscosity
π	3.1428
ρ	density
ρ_s	sediment density
σ_I	Inclusive Graphic Standard Deviation
τ_0	bed shear stress

APPENDIX B

Orifice Calibration

The orifice was calibrated by using a standard equation (equation (11)) for a sharp edges orifice with flange taps.

$$U_{y_0} b = 0.0438 d_o^2 c \sqrt{h_m} \quad \text{ft}^3/\text{sec} \quad (11)$$

where

d_o = orifice opening

h_m = difference in heights between legs of manometer

C is a factor which is a function of the flow Reynolds Number

ρ is the water density based on $T = 70$ °F.

c is a constant when $Re > 10^5$. The flows for this study were all in the region $Re < 10^5$ so that equation (11) had to be solved by interpolation with a Re vs. c graph. The result is shown in Fig. 32.

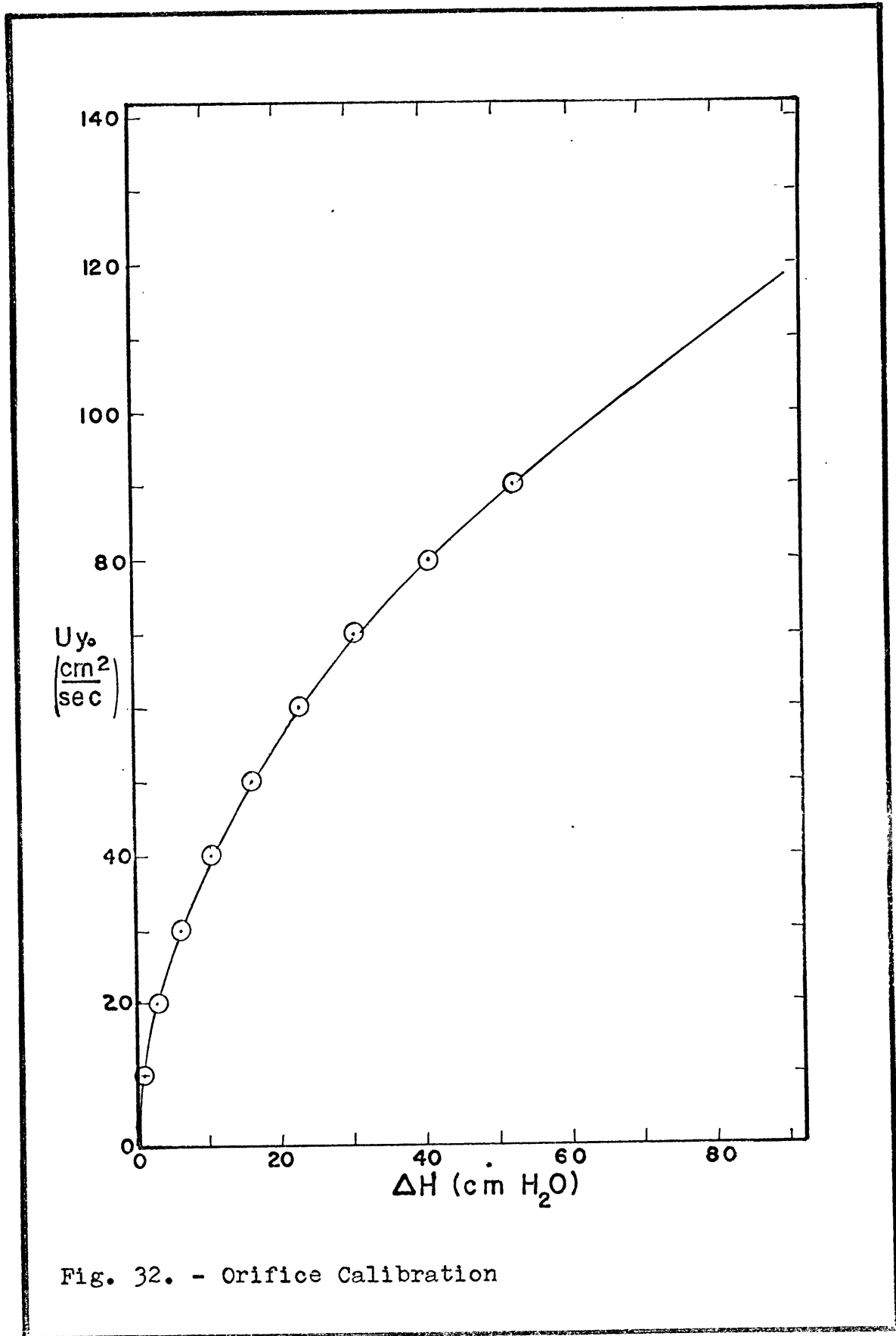


Fig. 32. - Orifice Calibration

APPENDIX C

Summary of Data

Table 3 - Run 1

t (min)	x_i (m), h_i (cm)					
	x_0	h_0	x_1	h_1	x_2	h_2
0	3.034	0.34				
5	3.059	0.26	3.114	0.07		
10	3.067	0.26	3.131	0.12		
15	3.073	0.25	3.144	0.23		
20	3.077	0.25	3.156	0.25	3.218	0.01
30	3.083	0.27	3.172	0.33	3.242	0.15
40	3.089	0.28	3.183	0.40	3.263	0.26
50	3.094	0.28	3.194	0.45	3.280	0.36
60	3.098	0.29	3.203	0.47	3.295	0.49
70	3.101	0.30	3.210	0.50	3.307	0.52
80	3.105	0.30	3.218	0.53	3.318	0.58
90	3.107	0.33	3.223	0.58	3.329	0.66
t	x_3	h_3	x_4	h_4	x_5	h_5
0						
5						
10						
15						
20						
30						
40	3.327	0.01				
50	3.354	0.17				
60	3.378	0.39	3.442	0.15		
70	3.396	0.52	3.420	0.35	3.354	0.24
80	3.414	0.65	3.499	0.51	3.575	0.45
90	3.430	0.77	3.528	0.80	3.611	0.58
t	x_6	h_6	x_7	h_7	x_8	h_8
0						
5						
10						
15						
20						
30						
40						
50						
60						
70	3.575	0.04				
80	3.640	0.37	3.688	0.08		
90	3.685	0.47	3.745	0.38	3.791	0.10

Table 4 - Run 2

x_i (m), h_i (cm)						
t (min)	x_0	h_0	x_1	h_1	x_2	h_2
0	2.564	0.34				
8	2.578	0.26	2.637	0.02		
18	2.587	0.21	2.663	0.16		
25	2.598	0.23	2.681	0.25	2.745	0.11
32	2.608	0.26	2.695	0.36	2.773	0.28
45	2.617	0.27	2.713	0.44	2.800	0.46
55	2.624	0.28	2.725	0.47	2.819	0.51
65	2.629	0.27	2.737	0.48	2.835	0.60
78	2.635	0.28	2.751	0.48	2.854	0.68
88	2.636	0.29	2.756	0.52	2.861	0.72
t	x_3	h_3	x_4	h_4	x_5	h_5
8						
18						
25						
32	2.838	0.17				
45	2.877	0.41	2.950	0.39	3.014	0.30
55	2.903	0.55	2.983	0.47	3.058	0.44
65	2.928	0.78	3.015	0.63	3.097	0.49
78	2.959	0.87	3.066	0.78		
88						
t	x_6	h_6				
8						
18						
25						
32						
45	3.059	0.07				
55	3.128	0.37				
65	3.174	0.62				
78						
88						

Table 5 - Run 3

x_i (m), h_i (cm)						
t (min)	x_0	h_0	x_1	h_1	x_2	h_2
0	2.500	0.34				
5	2.524	0.26	2.577	0.08		
10	2.531	0.25	2.596	0.15		
15	2.537	0.24	2.609	0.20		
20	2.540	0.24	2.619	0.23	2.685	0.0
25	2.543	0.24	2.626	0.26	2.693	0.0
35	2.548	0.25	2.636	0.31	2.707	0.10
45	2.552	0.26	2.648	0.36	2.728	0.24
60	2.558	0.27	2.650	0.41	2.750	0.35
70	2.560	0.27	2.667	0.41	2.761	0.41
80	2.563	0.27	2.673	0.42	2.770	0.45
90	2.565	0.29	2.679	0.42	2.780	0.50
t	x_3	h_3	x_4	h_4	x_5	h_5
0						
5						
10						
15						
20						
25						
35						
45	2.774	0.0				
60	2.824	0.21				
70	2.843	0.33	2.909	0.13		
80	2.858	0.44	2.935	0.34	2.989	0.16
90	2.871	0.49	2.955	0.48	3.030	0.38
t	x_6	h_6	x_7	h_7		
0						
5						
10						
15						
20						
25						
35						
45						
60						
70						
80						
90	3.090	0.28	3.134	0.0		

Table 6 - Run 4

x_1 (m), h_1 (cm)						
t (min)	x_0	h_0	x_1	h_1	x_2	h_2
0	2.453	0.33				
10	2.465	0.30	2.521	0.06		
20	2.468	0.29	2.534	0.09		
30	2.473	0.27	2.540	0.13		
40	2.473	0.26	2.547	0.15		
50	2.474	0.26	2.553	0.15		
80	2.477	0.27	2.562	0.22		
100	2.479	0.28	2.567	0.22		
120	2.480	0.28	2.570	0.24		
140	2.480	0.29	2.573	0.26		
160	2.482	0.29	2.575	0.27		
240	2.483	0.29	2.586	0.38	2.662	0.03
270	2.484	0.30	2.590	0.39	2.672	0.12
300	2.484	0.30	2.593	0.41	2.681	0.20
330	2.485	0.31	2.597	0.42	2.690	0.29
390	2.486	0.32	2.603	0.45	2.708	0.43
420	2.487	0.32	2.605	0.47	2.715	0.48
450	2.487	0.33	2.607	0.46	2.720	0.52
480	2.487	0.32	2.608	0.47	2.725	0.55
510	2.487	0.33	2.609	0.49	2.731	0.59
t	x_3	h_3	x_4	h_4		
0						
10						
20						
30						
40						
50						
80						
100						
120						
140						
160						
240						
270						
300						
330						
390	2.791	0.05				
420	2.865	0.16				
450	2.817	0.25				
480	2.831	0.34	2.917	0.0		
510	2.844	0.39	2.932	0.0		

Table 7 - Run 5

t (min)	x_i (m), h_i (cm)					
	x_0	h_0	x_1	h_1	x_2	h_2
0	2.453	0.35				
10	2.463	0.39	2.528	0.02		
20	2.465	0.41	2.537	0.09		
30	2.467	0.41	2.546	0.14		
60	2.471	0.44	2.561	0.23		
90	2.475	0.43	2.572	0.31		
120	2.478	0.44	2.582	0.36	2.659	0.12
150	2.480	0.44	2.589	0.40	2.676	0.25
180	2.483	0.45	2.596	0.45	2.692	0.48
210	2.484	0.44	2.602	0.50	2.703	0.44
240	2.487	0.42	2.607	0.53	2.711	0.52
270	2.488	0.43	2.611	0.57	2.721	0.58
450	2.500	0.44	2.637	0.59	2.771	0.58
t	x_3	h_3	x_4	h_4	x_5	h_5
0						
10						
20						
30						
60						
90						
120						
150	2.738	0.0				
180	2.767	0.14				
210	2.789	0.34				
240	2.806	0.45	2.884	0.23		
270	2.822	0.57	2.902	0.49	2.979	0.26
450	2.895	0.57	3.018	---	3.146	---

Table 8 - Run 6

t (min)	x_i (m), h_i (cm)					
	x_0	h_0	x_1	h_1	x_2	h_2
0	2.533	0.52				
15	2.541	0.46	2.616	0.12		
30	2.541	0.46	2.632	0.18		
45	2.541	0.47	2.641	0.21		
60	2.541	0.47	2.646	0.25		
77	2.542	0.46	2.651	0.24		
90	2.542	0.46	2.563	0.27		
105	2.542	0.46	2.656	0.29	2.719	0.0
120	2.542	0.45	2.659	0.30	2.738	0.06
150	2.542	0.45	2.663	0.32	2.747	0.19
180	2.542	0.44	2.667	0.32	2.760	0.28
210	2.543	0.43	2.670	0.38	2.770	0.36
240	2.543	0.43	2.673	0.36	2.777	0.40
300	2.543	0.42	2.678	0.38	2.790	0.50
360	2.543	0.42	2.682	0.41	2.802	0.54
t	x_3	h_3	x_4	h_4	x_5	h_5
0						
15						
30						
45						
60						
77						
90						
105						
120						
150						
120						
150						
180						
210	2.839	0.07				
240	2.857	0.24				
300	2.890	0.45	2.966	0.25		
360	2.915	0.48	3.308	0.41	3.090	0.42
					x_6 3.158	0.15 h_6

Table 9 - Run 7

x_1 (m), h_1 (cm)						
t (min)	x_0	h_0	x_1	h_1	x_2	h_2
0	1.938	0.36				
7	1.956	0.33	2.024	0.12	2.034	0.0
20	1.966	0.26	2.054	0.18	2.119	0.13
34	1.974	0.26	2.069	0.27	2.152	0.30
46	1.977	0.29	2.078	0.34	2.167	0.38
55	1.979	0.29	2.085	0.35	2.178	0.41
66	1.976	0.33	2.086	0.44	2.183	0.51
t	x_3	h_3	x_4	h_4	x_5	h_5
0						
7						
20						
34	2.224	0.28	2.287	0.10		
46	2.249	0.43	2.322	0.32	2.377	0.21
55	2.264	0.47	2.344	0.50	2.421	0.53
66	2.275	0.54	2.362	0.56	2.448	0.57
t	x_6	h_6	x_7	h_7	x_8	h_8
0						
7						
20						
34						
46						
55	2.477	0.42	2.520	0.16		
66	2.533	0.55	2.606	0.49	2.657	0.44

Table 10 - Run 8

x_i (m), h_i (cm)						
t (min)	x_0	h_0	x_1	h_1	x_2	h_2
0	2.468	0.49				
10	2.503	0.34	2.589	0.23	2.635	0.04
17	2.508	0.31	2.607	0.33	2.675	0.26
30	2.512	0.32	2.628	0.37	2.720	0.42
43	2.516	0.33	2.643	0.42	2.752	0.44
64	2.521	0.29	2.665	0.48	2.799	0.33
t	x_3	h_3	x_4	h_4	x_5	h_5
0						
10						
17	2.727	0.15	2.765	0.14		
30	2.801	0.42	2.872	0.44	2.911	0.18
43	2.854	0.72	2.932	0.25	2.990	0.48
64	2.936	0.32	3.083	--	3.188	0.96
t	x_6	h_6	x_7	h_7	x_8	h_8
0						
10						
17						
30	2.946	0.12	2.973	0.01		
43	3.034	0.14	3.066	0.27	3.017	0.20
64	3.275	0.28	3.350	0.43	3.400	0.67

Table 11 - Run 9

		x_i (m), h_i (cm)				
t (min)	x_0	h_0	x_1	h_1	x_2	h_2
0	2.450	0.43				
5	2.474	0.43	2.549	0.24	2.604	0.09
10	2.486	0.44	2.572	0.35	2.642	0.29
15	2.496	0.40	2.590	0.40	2.665	0.40
20	2.503	0.42	2.604	0.46	2.690	0.55
25	2.509	0.44	2.620	0.53	2.714	0.62
30	2.512	0.43	2.627	0.50	2.732	0.56
t	x_3	h_3	x_4	h_4	x_5	h_5
0						
5						
10	2.703	0.11	2.738	0.01	2.732	0.01
15	2.733	0.26	2.793	0.31	2.846	0.15
20	2.762	0.29	2.827	0.39	2.892	0.37
25	2.794	0.63	2.864	0.35	2.931	0.37
30	2.816	0.37				
t	x_6	h_6	x_7	h_7	x_8	h_8
0						
5						
10						
15	2.874	0.01	2.931	0.02		
20	2.950	0.30	2.999	0.20	3.027	0.01
25	2.992	0.40	3.045	0.27	3.097	0.47
30						
t	x_9	h_9	x_{10}	h_{10}		
0						
5						
10						
15						
20						
25	3.145	0.15	3.177	0.06		
30						

Table 12 - Run 10

t (min)	x_i (m), h_i (cm)					
	x_0	h_0	x_1	h_1	x_2	h_2
0	2.482	0.26				
7	2.496	0.23	2.557	0.10		
23	2.506	0.21	2.584	0.19		
43	2.512	0.19	2.600	0.23	2.665	0.05
64	2.517	0.21	2.614	0.29	2.695	0.24
79	2.521	0.21	2.622	0.31	2.712	0.33
100	2.527	0.16	2.632	0.35	2.732	0.41
113	2.527	0.23	2.635	0.39	2.743	0.46
122	2.531	0.17	2.640	0.38	2.750	0.48
143	2.533	0.19	2.648	0.40	2.763	0.50
t	x_3	h_3	x_4	h_4	x_5	h_5
0						
7						
23						
43						
64	2.753	0.04				
79	2.789	0.27	2.844	0.04		
100	2.820	0.40	2.898	0.36	2.965	0.29
113	2.835	0.49	2.921	0.46	2.999	0.42
122	2.847	0.48	2.934	0.53	3.018	0.41
143	2.866	0.57	2.961	0.74	3.059	0.81
t	x_6	h_6	x_7	h_7	x_8	h_8
0						
7						
23						
43						
64						
79						
100	3.007	0.07				
113	3.074	0.38	3.138	0.29	3.182	0.12
122	3.100	0.41	3.174	0.40	3.238	0.35
143	3.153	0.58	3.236	0.51	3.312	0.51

BIBLIOGRAPHY

- American Society of Civil Engineers, Task Committee on Preparation of Sediment Manual, 1966, Sediment transportation mechanics: initiation of motion: Proc., Am. Soc. Civil Engr., Jour. Hyd. Div., v. 92, no. HY2, p. 291-314.
- Barton, J.R. and Lin, P.N., 1955, A study of the sediment transport in alluvial channels, Fort Collins, Colo., Colorado A. & M., Civil Engr. Dept. Report # 55JRB2, 43 p.
- Brooks, N.H., 1958, Mechanics of streams with movable beds of fine sand: Am. Soc. Civil Engrs., Trans., v. 123, p. 526 - 594.
- Chien, N., 1956, The present status of research on sediment transport: Am. Soc. Civil Engrs., Trans., v. 121, p. 833-868.
- Colby, B.R., 1961, Effect of depth of flow on discharge of bed material: U.S. Geol. Surv., Water Supply Paper 1498-D.
- Einstein, H.A., 1942, Formulas for the transportation of bed load: Am. Soc. Civil Engrs., Trans., v. 107, p. 561-597.
- Folk, R.L., 1961, Petrology of sedimentary rocks, Austin, Texas, Hemphill's, 159 p.
- Gilbert, G.K., 1914, Transportation of debris by running water: U.S. Geol. Surv., Prof. Paper 86, 262 p.

- Hill, H.M., 1965, Bed forms due to a fluid stream: Proc., Am. Soc. Civil Engrs., Jour. Hyd. Div., v. 9, no. HY2, p. 127-144.
- Inman, D.L. and Bowen, A.J., 1963, Flume experiments on sand transport by waves and currents: in Proc. of 8th Conf. on Coastal Eng., J.W. Johnson, ed., Council on Naval Research, the Eng. Foundation, p. 137-150.
- Jopling, A.V., 1965, Hydraulic factors controlling the shape of laminae in laboratory deltas: J. Sediment. Petrol., v. 35, p. 777-791.
- Kennedy, J.F., 1963, The mechanics of dunes and antidunes in erodible-bed channels, J. Fluid Mech., v. 16, p. 521-544.
- Liu, H.K., 1957, Mechanics of sediment ripple formation: Proc., Am. Soc. Civil Engrs., v. 83, no. HY2, p. 1-23.
- Plate, E.J., 1957, Laboratory studies of the beginning of sediment ripple formation in an alluvial channel: M.S. thesis, Colorado State U., Fort Collins, Colo.
- Raichlen, F. and Kennedy, J.F., 1965, The growth of sediment bed forms from an initially flattened bed: International Assoc. for Hydraulic Research, Eleventh Intl. Congress, Leningrad, paper 3.7.
- Rathbun, R.E. and Guy, H.P., 1967, Measurement of hydraulic and sediment transport variables in a small recirculating flume: U.S. Geol. Surv., Water Resources Research, v. 3, #1, p. 107-122.

- Raudkivi, A.J., 1963, Study of sediment ripple formation:
Proc., Am. Soc. Civil Engrs., Jour. Hyd. Div., v. 89,
no. HY2, p. 1 - 23.
- Rubey, W.W., 1948, The forces required to move particles
on a stream bed: U.S. Geol. Surv., Prof. Paper 189E,
p. 121-142.
- Schlichting, H., 1960, Boundary layer theory, New York,
McGraw-Hill.
- Shields, A., 1936, Anwendung der Ahnlichkeitsmechanik und
der turbulenzforschung auf die Geschiebebewegung;
Berlin, Preussich Versuchanstalt fur Wasserbau and
Schiffbau, Mitteilungen, Heft 26.
- Simons, D.B. and Richardson, E.V., 1962, Resistance to
flow in alluvial channels: Am. Soc. Civil Engrs., Trans.,
v. 127, p. 927-954.
- Sutherland, A.J. and Hwang, L.S., 1965, A study of dune
geometry and dune growth: W.M. Keck Lab. of Hydr.
and Water Res., Tech. memo 65-5, 35 p.
- White, C.M., 1940, The equilibrium of grains on the bed
of an alluvial channel: Proc., Roy. Soc. (London),
Ser. A, vol 174, p. 322-338.